The Plant Cell, Vol. 20: 452–470, February 2008, www.plantcell.org © 2008 American Society of Plant Biologists

Tocopherols Modulate Extraplastidic Polyunsaturated Fatty Acid Metabolism in *Arabidopsis* at Low Temperature [W]

Hiroshi Maeda,[a,b,1] Tammy L. Sage,[c] Giorgis Isaac,[d] Ruth Welti,[d] and Dean DellaPenna[a,b,2]

[a] Department of Biochemistry and Molecular Biology, Michigan State University, East Lansing, Michigan 48824
[b] Cell and Molecular Biology Program, Michigan State University, East Lansing, Michigan 48824
[c] Department of Ecology and Evolutionary Biology, University of Toronto, Toronto, Ontario, Canada M5S 3B2
[d] Kansas Lipidomics Research Center, Division of Biology, Kansas State University, Manhattan, Kansas 66506

Tocopherols (vitamin E) are synthesized in plastids and have long been assumed to have essential functions restricted to these organelles. We previously reported that the *vitamin e-deficient2* (*vte2*) mutant of *Arabidopsis thaliana* is defective in transfer cell wall development and photoassimilate transport at low temperature (LT). Here, we demonstrate that LT-treated *vte2* has a distinct composition of polyunsaturated fatty acids (PUFAs): lower levels of linolenic acid (18:3) and higher levels of linoleic acid (18:2) compared with the wild type. Enhanced 18:3 oxidation was not involved, as indicated by the limited differences in oxidized lipid species between LT-treated *vte2* and the wild type and by a lack of impact on the LT-induced *vte2* phenotype in a *vte2 fad3 fad7 fad8* quadruple mutant deficient in 18:3. PUFA changes in LT-treated *vte2* occur primarily in phospholipids due to reduced conversion of dienoic to trienoic fatty acids in the endoplasmic reticulum (ER) pathway. Introduction of the ER *fatty acid desaturase* mutation, *fad2*, and to a lesser extent the plastidic *fad6* mutation into the *vte2* background suppressed the LT-induced *vte2* phenotypes, including abnormal transfer cell wall development. These results provide biochemical and genetic evidence that plastid-synthesized tocopherols modulate ER PUFA metabolism early in the LT adaptation response of *Arabidopsis*.

INTRODUCTION

Tocopherols were first discovered as an essential dietary nutrient for mammals and, together with tocotrienols, are collectively known as vitamin E (Evans and Bishop, 1922; Bramley et al., 2000; Schneider, 2005). Based on in vitro studies, these lipid-soluble compounds are effective antioxidants that quench singlet oxygen and scavenge lipid peroxyl radicals and hence terminate the autocatalytic chain reaction of lipid peroxidation (Tappel, 1972; Fahrenholtz et al., 1974; Burton and Ingold, 1981; Liebler and Burr, 1992; Kamal-Eldin and Appelqvist, 1996). Tocopherols localize in membranes where they associate with polyunsaturated fatty acids (PUFAs) and affect properties such as the permeability and stability of membranes (Erin et al., 1984; Kagan, 1989; Stillwell et al., 1996; Wang and Quinn, 2000).

In animals, tocopherol deficiency has severe consequences, including neurological dysfunction and muscular dystrophy (Bramley et al., 2000; Schneider, 2005). Because tocopherol deficiency symptoms are often associated with increased oxidative stresses, it has been generally accepted that tocopherols primarily function as antioxidants in animal membranes. Studies with mammalian cell cultures have led to the proposal that specific forms of tocopherols (e.g., α-tocopherol but not γ-tocopherol) also have functions unrelated to their antioxidant properties, which include modulation of signaling pathways (Pentland et al., 1992; Ricciarelli et al., 1998, 2002; Jiang et al., 2000; Rimbach et al., 2002). However, the underlying mechanisms of tocopherol function(s) in animals remain an open question.

Despite the fact that tocopherols are synthesized only by photosynthetic organisms, including all plants and algae and some cyanobacteria, until recently there was no direct evidence demonstrating the roles of tocopherols in photosynthetic organisms (Fryer, 1992; Munne-Bosch and Alegre, 2002; Maeda and DellaPenna, 2007). The tocopherol-deficient *vte2* (for *vitamin e2*) mutant of *Arabidopsis thaliana* is defective in homogentisate phytyl transferase, the first committed enzyme of the tocopherol biosynthetic pathway (Collakova and DellaPenna, 2001, 2003; Savidge et al., 2002), and lacks all tocopherols and pathway intermediates (Sattler et al., 2004). The *vte2* mutant has reduced seed viability and impaired seedling development, both of which are associated with a massive elevation in lipid peroxidation (Sattler et al., 2004, 2006), indicating that tocopherols play an essential role as lipid-soluble antioxidants during seed dormancy and early seedling development. However, mature *vte2* plants and the orthologous mutant in *Synechocystis* sp PCC6803 (Collakova and DellaPenna, 2001; Savidge et al., 2002) were virtually indistinguishable from their respective wild types under normal growth conditions and also during high intensity light stress (Sattler et al., 2004; Maeda et al., 2006; Sakuragi et al., 2006). They became distinguishable only under combinations of

[1] Current address: Department of Horticulture and Landscape Architecture, Purdue University, 625 Agriculture Mall Dr., West Lafayette, IN 47907.
[2] Address correspondence to dellapen@msu.edu.
The author responsible for distribution of materials integral to the findings presented in this article in accordance with the policy described in the Instructions for Authors (www.plantcell.org) is: Dean DellaPenna (dellapen@msu.edu).
[W] Online version contains Web-only data.
www.plantcell.org/cgi/doi/10.1105/tpc.107.054718

high light and low temperature or lipid peroxidation-inducing chemical treatment (Havaux et al., 2005; Maeda et al., 2005, 2006). These results suggest a more limited role of tocopherols in high light stress than had been assumed.

In contrast with the lack of a visible phenotype in *Arabidopsis* tocopherol-deficient mutants under normal growth and high light stress conditions, tocopherol-deficient maize (*Zea mays*) and potato (*Solanum tuberosum*) plants had reduced stature and massive carbohydrate and anthocyanin accumulation in source leaves, suggesting impairment of photoassimilate transport (Russin et al., 1996; Provencher et al., 2001; Hofius et al., 2004). Most recently, a similar carbohydrate and anthocyanin accumulation phenotype was also observed in tocopherol-deficient *Arabidopsis vte2* mutants in response to nonfreezing low-temperature (LT) treatment (i.e., 3 to 12°C; Maeda et al., 2006). As early as 6 h after transfer to LT, tocopherol deficiency in *vte2* resulted in abnormal callose deposition and defective transfer cell wall development in phloem parenchyma cells, either one or both of which creates a bottleneck for photoassimilate export from source tissues. The resulting inhibition of photoassimilate export subsequently leads to carbohydrate and anthocyanin accumulation after 3 and 14 d, respectively, and to growth inhibition of whole plants after 1 month of LT treatment (Maeda et al., 2006). Notably, the LT phenotypes of *vte2* were independent of light level and not associated with markers of photooxidative stress (Maeda et al., 2006). These combined results from tocopherol-deficient plants demonstrated a crucial role for tocopherols in phloem loading for photoassimilate export.

Given the well-characterized chemical nature of tocopherols as lipid-soluble antioxidants (Tappel, 1972; Liebler and Burr, 1992; Kamal-Eldin and Appelqvist, 1996) and their localization in PUFA-enriched chloroplast membranes (Bucke, 1968; Soll et al., 1985; Wise and Naylor, 1987), we hypothesized that tocopherol deficiency in *Arabidopsis* impacts chloroplast membrane lipids and that this might be an underlying cause of the impaired phloem loading phenotype of tocopherol-deficient plants. In this study, we conducted a detailed analysis of membrane lipid oxidation, composition, and dynamics during LT treatment of *vte2* and the wild type and found that tocopherol deficiency has a major impact on PUFA composition not due to elevated lipid peroxidation in plastids but rather because of altered PUFA synthesis in the endoplasmic reticulum (ER).

RESULTS

vte2 and the Wild Type Have Distinct Dienoic and Trienoic Fatty Acid Levels at LT

To examine if tocopherol deficiency affects fatty acid composition of *Arabidopsis* leaves, *vte2* and Columbia (Col) plants were grown under permissive conditions (22°C) for 4 weeks and the middle portion of fully expanded rosette leaves harvested and analyzed. The total fatty acid composition of Col and *vte2* leaves grown at permissive conditions was indistinguishable (Figure 1). Because tocopherol deficiency has a dramatic impact on LT adaptation of *Arabidopsis* (Maeda et al., 2006), we hypothesized that tocopherol deficiency would affect membrane lipid composition at LT. To test this possibility, 4-week-old *vte2* and Col plants grown at 22°C were transferred to LT (7°C) conditions and leaf total fatty acid compositions were compared after 14 d of LT treatment. Col had higher α-linolenic acid (18:3) at 7°C than it did at 22°C, as reported previously (Williams et al., 1988). Interestingly, LT-treated *vte2* had significantly higher linoleic acid (18:2) and correspondingly lower 18:3 relative to Col (Figure 1).

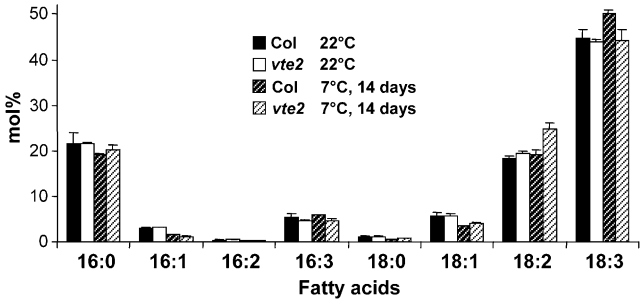

Figure 1. Total Fatty Acid Composition of Col and *vte2* Leaves before and after 14 d of LT Treatment.

Col and *vte2* plants were grown at 22°C for 4 weeks, and the middle portions of mature leaf blades were harvested for analysis before and after 14 d of 7°C treatment. Values for each fatty acid (x:y represents number of carbons:number of unsaturated bonds) are means ± SD ($n = 4$ biological replicates) and are expressed as mol %.

PUFA Changes in LT-Treated *vte2* Are Temporally and Spatially Associated with Vascular-Specific Callose Deposition

As previously reported, after transfer to LT, *vte2* accumulated callose initially in petiole vascular tissue and subsequently in an acropetal fashion throughout leaf blade vascular tissue (Maeda et al., 2006). The timing of this response suggested that vascular-specific callose deposition is an early response of the *vte2* LT-induced phenotypes. To assess if LT-induced, *vte2*-dependent PUFA alterations are related to vascular-specific callose deposition, tissue from the petiole and mid-blade of mature leaves was harvested after 0, 3, 7, and 14 d of LT treatment, and total fatty acid composition and aniline blue–positive fluorescence, a measure of callose deposition, were compared. Consistent with the results from Figure 1, *vte2* mid-blades in comparison to Col showed lower 18:3 and higher 18:2 levels in response to LT and, as a result, a significantly lower 18:3/18:2 ratio after 7 d of LT treatment (Figure 2A; see Supplemental Table 1 online). In *vte2* mid-blades, only a few weak aniline blue–positive fluorescence spots were detected at 3 d, and their frequency and intensity dramatically increased by 7 d (Figure 2B). No fluorescence was detected in Col leaf blades and petioles at all time points (Maeda et al., 2006). Thus, PUFA alterations appear temporally correlated with callose deposition in *vte2* leaf blades during LT treatment. When 18:2 and 18:3 levels were analyzed from the petioles of *vte2* and Col plants, significant differences in 18:3/18:2 ratios were observed even before LT treatment (Figure 2A), whereas aniline blue–positive fluorescence in *vte2* petioles first became apparent after 6 h of LT treatment (Maeda et al., 2006) and was strongly elevated by 3 d of LT treatment (Figure 2B). This

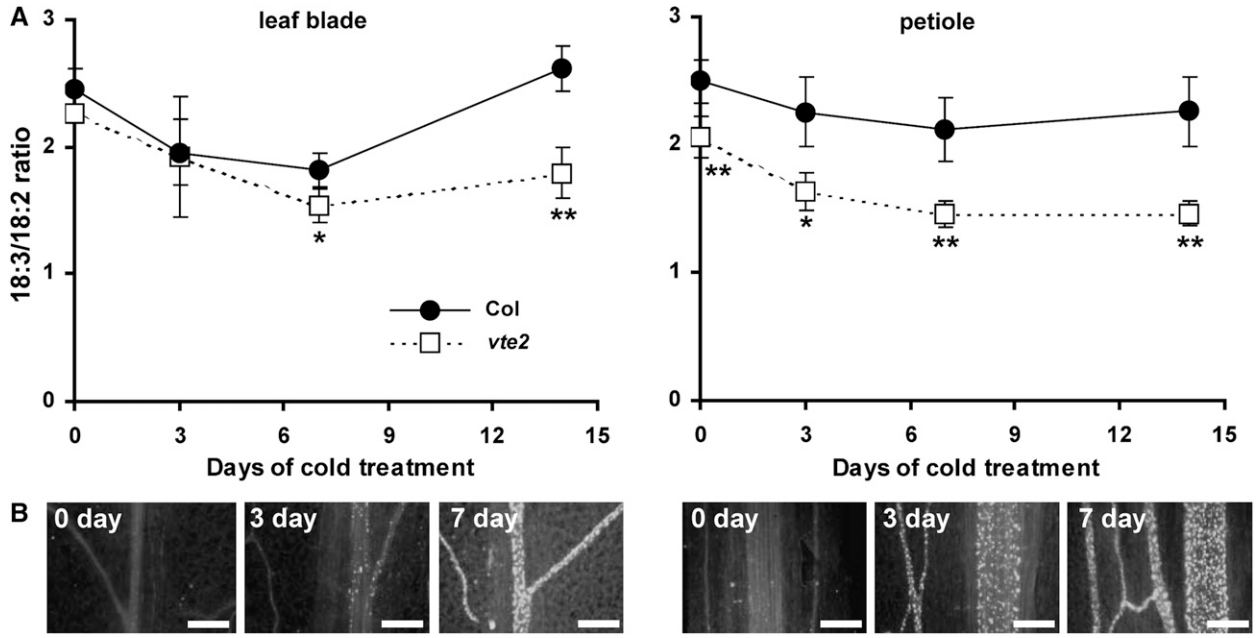

Figure 2. 18:3/18:2 Ratio and Callose Deposition in the Petioles and Leaf Blades of Col and *vte2* during LT Treatment.

Col and *vte2* plants were grown at 22°C for 4 weeks and then transferred to 7°C for an additional 14 d.

(A) Fatty acid composition of total lipid extracts was analyzed from the middle portions of leaf blades (left graph) and petioles (right graph) of Col (closed circles) and *vte2* (open squares). Data are means ± SD ($n = 4$ biological replicates). Asterisks represent significance levels using Student's *t* test of *vte2* relative to Col at each time point (* $P < 0.05$; ** $P < 0.01$).

(B) Aniline blue–positive fluorescence of *vte2* leaf blades (left) and petioles (right) of *vte2* after 0, 3, and 7 d of LT treatment. Bars = 100 μm.

result indicates that *vte2*-specific PUFA alterations occur in petioles prior to callose deposition and the onset of other *vte2* LT phenotypes.

The *vte2* Mutation Impacts PUFAs Derived from the ER Pathway at LT

To further examine changes in membrane lipid composition in *vte2*, individual lipid molecular species were analyzed before and after 14 d of LT treatment using electrospray ionization triple quadrupole mass spectrometry (MS; Welti et al., 2002; Welti and Wang, 2004; Devaiah et al., 2006). Under permissive conditions, the levels of polar lipid classes (leaf 22°C in Figure 3A) and the composition of fatty acids esterified to each polar lipid class (leaf 22°C in Figure 3B) were similar in *vte2* and Col leaves, indicating that tocopherol deficiency per se does not impact the membrane lipid and fatty acid composition of *Arabidopsis* leaves under permissive growth conditions.

After 14 d of LT treatment, the head-group composition of polar lipid classes was also similar between *vte2* and Col (leaf 7°C in Figure 3A), whereas the fatty acid composition of each polar lipid class exhibited distinct changes especially in 18:3- and 18:2-containing acyl species (leaf 7°C in Figure 3B). Digalactosyldiacylglycerol (DGDG) in *vte2* relative to Col had higher 34:3 and lower 36:6 species, which mainly consist of pairs of 16:0 and 18:3 fatty acids (hereafter indicated as 16:0-18:3) and 18:3-18:3, respectively, in *Arabidopsis* leaf (Figure 3B; Marechal et al., 1997; Welti et al., 2002). Monogalactosyldiacylglycerol (MGDG) in *vte2* had lower 36:6 (18:3-18:3) and higher 34:6 (18:3-16:3) compared with Col. Unexpectedly, the fatty acid composition of two major phospholipids, phosphatidylcholine (PC) and phosphatidylethanolamine (PE), were strongly impacted by the *vte2* mutation. The mutant in comparison to Col had lower 36:6 (18:3-18:3) and 34:3 (16:0-18:3) and higher 36:4 (18:2-18:2) and 34:2 (16:0-18:2) in both PC and PE (Figure 3B). These data were in accordance with the decreased level of 18:3 in total fatty acid analysis of LT-treated *vte2* relative to Col (Figure 1).

The levels of individual lipid molecular species were also analyzed from the petioles of 3-d LT-treated *vte2* and Col plants. As observed in 14-d LT-treated leaves, the composition of polar lipid classes was similar between 3-d LT-treated *vte2* and Col petioles (petiole 7°C in Figure 3A). The 36:6 (18:3-18:3) and 34:3 (16:0-18:3) acyl species of PC and PE were reduced, and 36:4 (18:2-18:2) and 34:2 (16:0-18:2) species were increased in the petioles of *vte2* relative to Col (petiole 7°C in Figure 3B). However, unlike 14-d LT-treated leaves, the composition of fatty acids esterified to MGDG and DGDG was similar between genotypes in 3-d LT-treated petiole. These results indicate that the molecular species consistently decreased in the leaves and petioles of LT-treated *vte2* in comparison to Col (i.e., 18:3-18:3 and 16:0-18:3 acyl pairs of PC and PE) are all derived from the ER pathway (Figure 3C) and suggest that tocopherol deficiency at LT primarily reduces the level of 18:3 derived from the ER pathway.

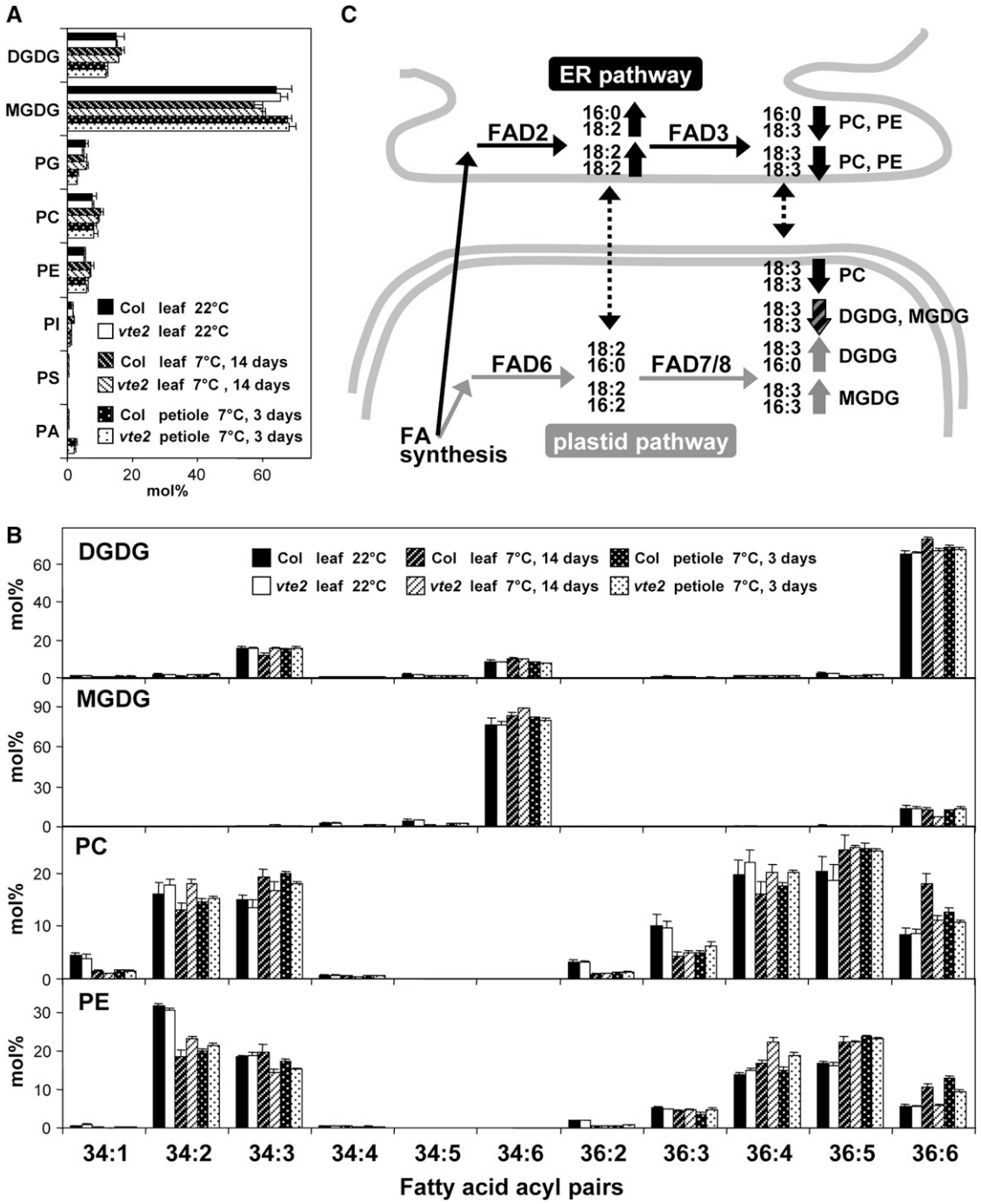

Figure 3. Lipid Profiles of Col and *vte2* Leaves and Petioles before and after 14 d of LT Treatment.

(A) and **(B)** Col and *vte2* were grown at 22°C for 4 weeks and then transferred to 7°C. Black and white bars are Col and *vte2* leaves, respectively, before LT treatment. White-hatched and black-hatched bars are Col and *vte2* leaves, respectively, after 14 d of LT treatment. White-dotted and black-dotted bars are Col and *vte2* petioles, respectively, after 3 d of LT treatment. Values are means ± SD ($n = 5$ biological replicates) and are expressed as mol %. PI, phosphatidylinositol; PS, phosphatidylserine; PA, phosphatidic acid; FA, fatty acid.

(A) Mole percent of total polar lipid classes analyzed.

(B) Mole percent of fatty acids esterified to DGDG, MGDG, PC, and PE.

(C) A diagram summarizing membrane PUFA biosynthesis in *Arabidopsis* and the PUFA-containing lipid molecular species (e.g., PC and PE with 16:0 and 18:3 acyls shown at the right top corner) that are higher (up arrows) and lower (down arrows) in LT-treated *vte2* relative to Col. Black and gray arrows indicate acyl pairs derived from the ER and plastid pathways, respectively, while the striped arrow indicates lipid species that can be produced from both pathways. Dotted arrows illustrate proposed transfer of lipids between the ER and plastid.

Oxidized Membrane Lipid Species Are Not Elevated in LT-Treated *vte2*

How does the absence of tocopherols in *vte2* lead to lower 18:3 compared with Col at LT? Given the well-established roles of tocopherols as lipid-soluble antioxidants and the massive increase in the levels of lipid oxidation products in germinating *vte2* seedlings (Sattler et al., 2004, 2006), peroxidation of PUFAs, especially 18:3, in LT-treated *vte2* would seem an obvious explanation. Though a prior report found no differences in the level of lipid-soluble peroxides accumulated in LT-treated Col and *vte2* as detected by the ferrous oxidation xylenol orange assay (FOX assay; Maeda et al., 2006), if the lipid peroxides in LT-treated *vte2* plants were rapidly converted to other oxylipins, they would not be detectable by the FOX assay. To test this possibility, total lipids were extracted from 3-d LT-treated *vte2* and Col petioles, where the most rapid and obvious fatty acid composition differences were observed between genotypes (Figures 2 and 3), and oxygenated 18-carbon acyls esterified to galactolipids (MGDG and DGDG) and phospholipids (PC, PE, and phosphatidylglycerol [PG]) were analyzed.

Nominal masses that correspond nearly uniquely to oxidized 18-carbon acyl chains were identified using quadrupole time-of-flight (Q-TOF; details in Methods and Supplemental Figure 1 online). These 18-carbon oxylipins include 18:2-O (18 carbons, two double-bond equivalents, and one oxygen in addition to the carbonyl oxygen), 18:3-O, 18:4-O, 18:2-2O, and 18:3-2O. 18:2-O could correspond to hydroxy-octadienoic acid, 18:3-O to hydroxy-octatrienoic acid or keto-octadienoic acid, and 18:2-2O to hydroperoxy-octadienoic acid (Chechetkin et al., 2004; Montillet et al., 2004). 18:4-O and 18:3-2O in wounded *Arabidopsis* complex lipids have been implicated to be oxophytodienoic acid (OPDA) and either α or γ ketol, respectively (Buseman et al., 2006), but could also correspond to keto-octatrienoic acid (KOTE; structure illustrated in Blée and Joyard, 1996) and hydroperoxy-octatrienoic acid, respectively. Anionic acyl fragment masses corresponding to these oxygenated 18 carbon acyls were identified on PC, PE, PG, MGDG, and DGDG molecular species using triple quadrupole MS.

A total of 34 oxidized complex lipid molecular species were detected (see Supplemental Figure 1 online). However, the levels of most oxidized complex lipid species were quite low and not different between genotypes (Figure 4; see Supplemental Figure 1 online). Compared with samples subjected to more severe stresses (e.g., wounding), the LT-treated petioles had much less oxidized complex lipid (Buseman et al., 2006). Although this analysis does not provide one-to-one identification between a detected ion and an individual compound (e.g., 18:4-O could be either OPDA or 13-KOTE), these results indicate that membrane lipid oxidation is not occurring at significantly elevated or different levels in LT-treated *vte2* and Col and that the lower level of 18:3 in *vte2* relative to Col is not due to elevated oxidation of 18:3.

In Vivo Conversion of ER-Derived Dienoic to Trienoic Fatty Acids Is Reduced in LT-Treated *vte2*

Lipid profiling data and oxidized lipid analysis suggested that tocopherol deficiency in *vte2* impacts 18:3 synthesis in the ER

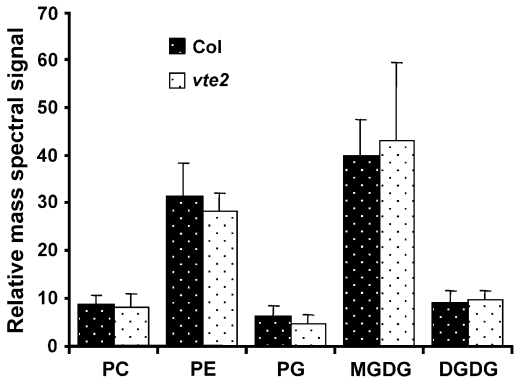

Figure 4. Oxylipin-Containing Polar Lipid Species in 3-d LT-Treated Col and *vte2* Petioles.

Compounds containing 18-carbon oxygenated fatty acyl anions were analyzed by mass spectrometry as described in Methods. White- and black-dotted bars are Col and *vte2* petioles, respectively, after 3 d of LT treatment. Data include 34 molecular species (9 PC, 10 PE, 3 PG, 7 MGDG, and 5 DGDG) with oxygenated 18-carbon fatty acids; details about the analyzed species are given in Supplemental Figure 1 online. Values are means ± SD ($n = 5$ biological replicates). No significant differences were observed in all cases between genotypes (Student's *t* test, $P > 0.05$).

pathway at LT. To directly test this possibility, lipid biosynthesis in *vte2* and Col was examined under permissive and LT conditions using radiolabel tracer experiments. To assess early impacts of tocopherol deficiency on lipid metabolism during LT treatment, Col and *vte2* leaves were labeled with [^{14}C]-acetate at 22°C for 2 h and then transferred to 7°C (or kept at 22°C for controls). The redistribution of radioactivity into different fatty acids was examined for an additional 8 d as described previously (Morris, 1966; Browse et al., 1986b). After 2 h of labeling at 22°C, radioactivity was almost equally distributed into saturated, monoenoic, dienoic, and trienoic fatty acids (see initial time points in Figure 5A). When kept at 22°C, incorporation of radioactivity into trienoic fatty acids gradually increased to nearly 70% of total activity, and incorporation into saturated, monoenoic, and dienoic fatty acids correspondingly decreased. These labeling patterns were almost identical between Col and *vte2* (Figure 5A).

When transferred to 7°C, *vte2* in comparison to Col incorporated less radioactivity into trienoic fatty acids and more into dienoic fatty acids: after 192 h, *vte2* in comparison to Col incorporated 3.6% ± 1.7% less and 4.6% ± 1.3% more ^{14}C into trienoic and dienoic fatty acids, respectively ($P < 0.01$, $n = 3$; Figure 5A). Incorporation patterns into saturated and monoenoic fatty acids at 7°C were similar between genotypes: *vte2* in comparison to Col incorporated 0.4% ± 0.5% and 0.5% ± 1.1% less ^{14}C into monoenoic and saturated fatty acids, respectively, at 192 h ($P > 0.05$, $n = 3$). In a separate set of experiments, plants were treated at 7°C for 3 d prior to labeling at 7°C and the redistribution of radioactivity was examined. Under these conditions, *vte2* incorporated even less radioactivity into trienoic fatty acids and more into dienoic fatty acids in comparison to Col (13.0% less and 10.3% more, respectively; see Supplemental Figure 2A online). These results indicate that tocopherol

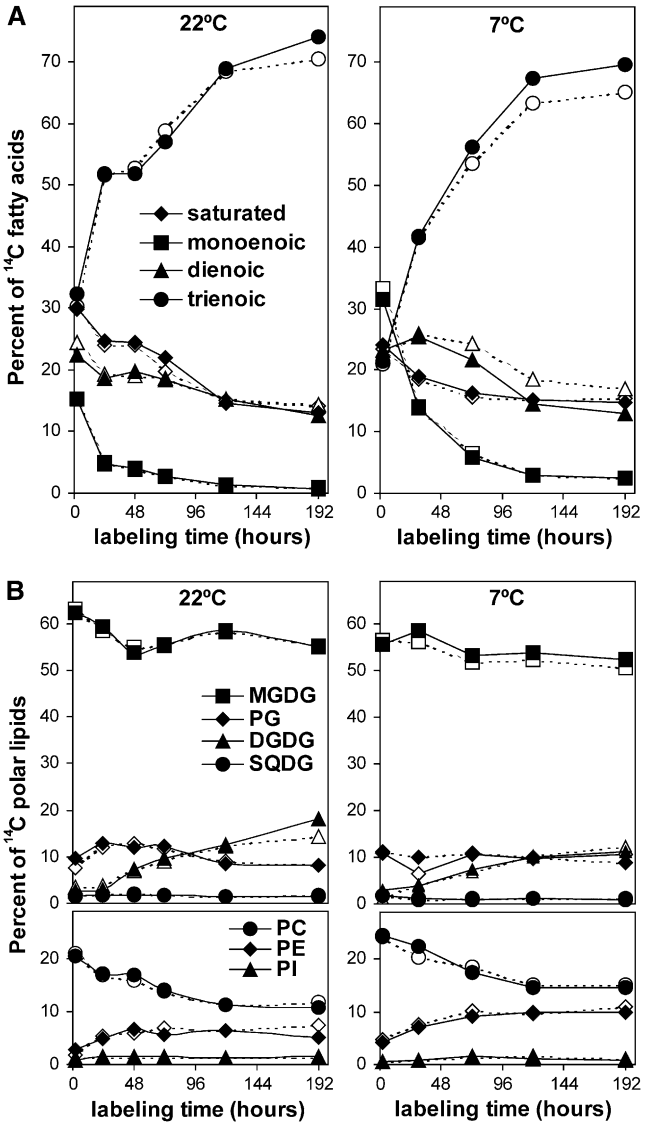

Figure 5. Redistribution of Radioactivity among the Fatty Acids and Polar Lipids of Col and *vte2* at 22 or 7°C.

Col (closed symbols) and *vte2* (open symbols) were grown at 22°C for 4 weeks, labeled with [^{14}C]-acetate at 22°C at time zero, and harvested for the first time point 2 h later, after which time the labeled plants were either kept at 22°C (left graphs) or transferred to 7°C (right graphs) for the indicated times. All experiments were repeated three times with similar trends. Representative data are shown.

(A) Redistribution of radioactivity among individual fatty acids. diamonds, saturated; squares, monoenoic; triangles, dienoic; circles, trienoic fatty acids.

(B) Redistribution of radioactivity among individual polar lipids. Top panels: squares, MGDG; diamonds, PG; triangles, DGDG; circles, SQDG (sulfoquinovosyldiacylglycerol). Bottom panels: circles, PC; diamonds, PE; triangles, PI.

deficiency negatively impacts the in vivo conversion of dienoic to trienoic fatty acids at LT.

The redistribution of radioactivity into different polar lipid classes was also examined by separating total lipid extracts of labeled leaves by thin layer chromatography (TLC). The MGDG, PC, and PE bands were recovered from the TLC plates and transmethylated and separated into different fatty acid methyl esters on argentation TLC. Col and *vte2* showed very similar labeling patterns into various lipid classes at both 22 and 7°C (Figure 5B). The labeling patterns into different fatty acids esterified to MGDG, PC, and PE was also very similar between Col and *vte2* when maintained at 22°C (Figure 6).

When transferred to 7°C, *vte2* and Col exhibited nearly identical labeling patterns of MGDG acyl species, but *vte2* incorporated less radioactivity into trienoic fatty acids and more into dienoic fatty acids esterified to PC and PE than did Col. For example, after 192 h, *vte2* incorporated 10.0% $\pm$ 3.0% less and 11.7% $\pm$ 3.7% more ^{14}C into trienoic and dienoic fatty acids of PC, respectively ($P < 0.01$, $n = 3$; Figure 6). Similar but more extreme trends were observed when plants were first LT-treated for 3 d before being labeled and maintained at 7°C (see Supplemental Figure 2C online). These results are in good agreement with steady state lipid composition analysis (Figure 3) and indicate that tocopherol deficiency at LT negatively impacts the in vivo conversion of dienoic to trienoic fatty acids esterified to PC and PE, both of which are produced through the ER pathway.

$^{14}CO_2$ labeling allows one to pulse label and chase (in ambient air) to follow the turnover of total fatty acids (Bonaventure et al., 2004), while [^{14}C]-acetate labeling does not. Col and *vte2* plants were labeled with a 30-min pulse of $^{14}CO_2$ and then chased in air for an additional 8 d. Leaf tissue was harvested at different time points, total membrane lipids were extracted and transmethylated, and the amount of radioactivity incorporated into total fatty acids was determined. The level of radioactivity in fatty acids increased during the first 7 h after labeling and gradually decreased thereafter (Figure 7). The slope of reduction of radioactivity in total fatty acids was similar between Col and *vte2* (Figure 7) even when corrected for the dilution effect caused by growth (see Supplemental Figure 3 online). These results suggest that Col and *vte2* turnover fatty acids at similar rates and that tocopherol deficiency does not significantly affect this process.

fad2 and *fad6*, But Not *fad3*, *fad7*, or *fad8*, Suppress the Impaired Photoassimilate Export Phenotype of LT-Treated *vte2*

To further examine the relationship between PUFA alterations and the LT-induced phenotype of *vte2*, a series of mutations affecting plastid- or ER-localized fatty acid desaturases were introduced into the *vte2* background and the consequences for the *vte2* LT phenotypes were assessed. In higher plants, PUFAs are synthesized through both prokaryotic (chloroplast) and eukaryotic (ER) pathways (Roughan et al., 1980; Browse et al., 1986b; Figure 3C). FAD2 and FAD3 are ER-localized fatty acid desaturases; thus, the *fad2* and *fad3* mutants have reduced PUFA content predominantly in phospholipids, the major lipid components of extraplastidic membranes (Miquel and Browse,

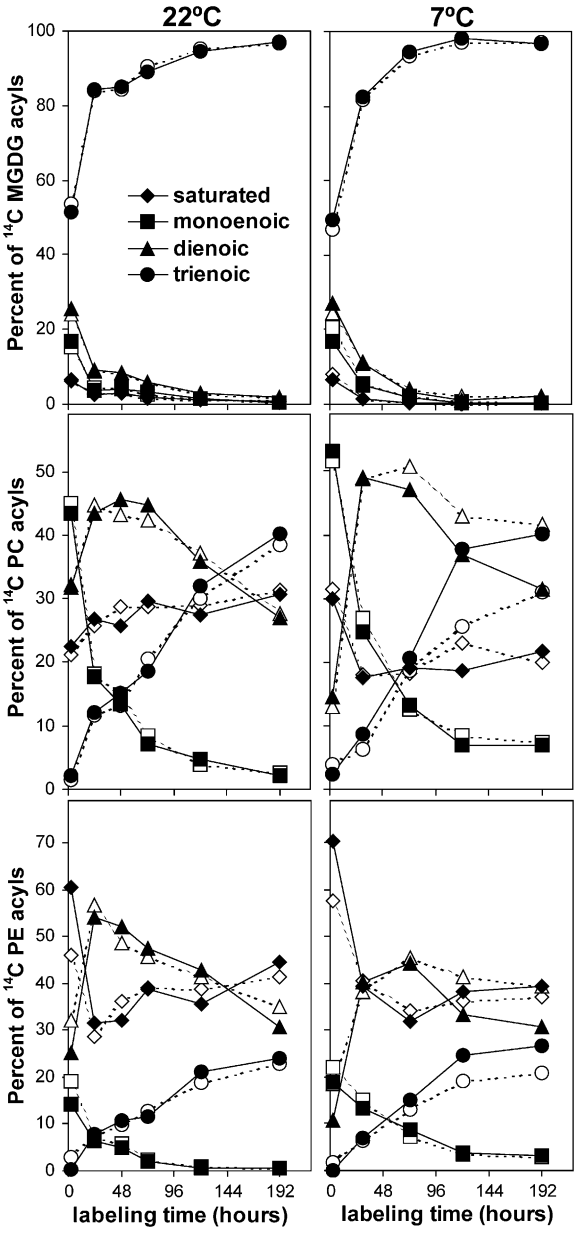

Figure 6. Redistribution of Radioactivity among Fatty Acids of Individual Lipids from Col and *vte2* at 22 or 7°C.

Col (closed symbols) and *vte2* (open symbols) were treated and labeled as in Figure 5. Redistribution of radioactivity among individual fatty acid methylesters of MGDG, PC, or PE was analyzed by TLC. All experiments were repeated three times, except for 7°C MGDG and PE, which were repeated two times. All experiments showed similar trends, and representative data are shown. For the 7°C experiment, an additional experiment was also conducted using 3-d LT-treated plants, and similar but more obvious trends were observed (see Supplemental Figure 2 online). Diamonds, saturated; squares, monoenoic; triangles, dienoic; circles, trienoic fatty acids.

1992; Browse et al., 1993; Okuley et al., 1994). FAD6, FAD7, and FAD8 are plastid-localized fatty acid desaturases, and the *fad6* and *fad7 fad8* mutants have reduced PUFAs predominantly in galactolipids, the major lipid components of plastidic membranes (Browse et al., 1989; Falcone et al., 1994; McConn et al., 1994). FAD2 and FAD6 convert monoenoic- to dienoic-fatty acids, whereas FAD3, FAD7, and FAD8 convert dienoic- to trienoic fatty acids; thus, compared with Col, the *fad2* and *fad6* mutants contain higher 18:1 and the *fad3*, *fad7*, and *fad8* have higher 18:2 and all these genotypes have lower 18:3 (Browse et al., 1989, 1993; Miquel and Browse, 1992; Falcone et al., 1994; McConn et al., 1994; Okuley et al., 1994; Wallis and Browse, 2002). The *fad3 fad7 fad8* triple mutant lacks all trienoic fatty acids (i.e., 18:3 and 16:3; McConn and Browse, 1996).

Under permissive growth conditions, the visible phenotype (see Supplemental Figure 4 online) and fatty acid composition (Table 1) of all *fad*-containing *vte2* mutant lines were visually indistinguishable from the corresponding single, double, or triple *fad* mutant parents. When 4-week-old plants grown at 22°C were transferred to 7°C conditions for an additional 4 weeks, the *fad2*, *fad6*, *fad3*, *fad7 fad8*, and *fad3 fad7 fad8* mutants were also indistinguishable from Col (Figure 8A). Although the *fad2*, *fad6*, and *fad3 fad7 fad8* mutants are known to be chilling sensitive, the plant age and conditions used for our LT treatment (see Methods) do not induce chilling sensitivity in these mutants (Hugly and Somerville, 1992; Miquel et al., 1993; Routaboul et al., 2000). The *vte2* mutant showed the expected LT-induced phenotype, and *vte2 fad3*, *vte2 fad7 fad8*, and *vte2 fad3 fad7 fad8* mutants exhibited a visible phenotype similar to *vte2* (Figure 8A).

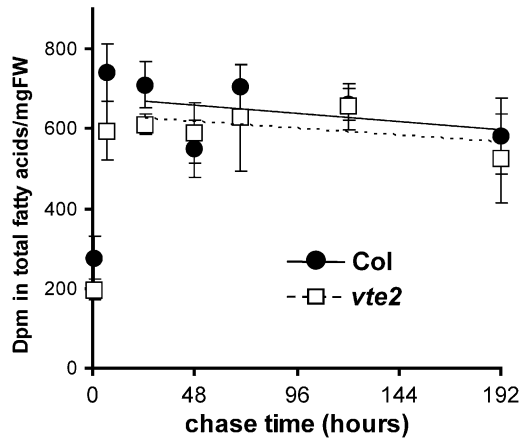

Figure 7. $^{14}CO_2$ Pulse Chase Labeling of Total Fatty Acids in LT-Treated Col and *vte2*.

Col (closed circles) and *vte2* (open squares) grown at 22°C for 3 weeks were transferred to 7°C for 3 d and then pulse labeled with $^{14}CO_2$ for 30 min and chased in air at 7°C. At the indicated times, leaf samples were harvested and the specific activity in total fatty acids determined. Samples for the initial time point were taken immediately after labeling (30 min). Values are means ± SD ($n = 3$ biological replicates) and are expressed as radioactivity detected in total fatty acids per mg fresh weight (FW). Estimated rates of fatty acid turnover are indicated as the slopes of solid (Col) and dotted (*vte2*) lines based on values starting at the 24-h time point.

Table 1. Fatty Acid Composition of Indicated Genotypes before and after 14 d of LT Treatment

Plant	16:0	16:1	16:2	16:3	18:0	18:1	18:2	18:3
Before LT treatment								
Col	16.6 ± 2.1	3.2 ± 0.4	0.6 ± 0.1	6.9 ± 1.0	1.1 ± 0.1	5.9 ± 0.5	17.8 ± 1.9	48.0 ± 3.5
vte2	15.9 ± 1.6	3.1 ± 0.4	0.6 ± 0.2	7.5 ± 1.4	1.0 ± 0.2	5.7 ± 1.2	17.6 ± 2.4	48.4 ± 4.3
fad2	17.4 ± 1.8	2.9 ± 0.6	0.5 ± 0.1	7.7 ± 1.4	0.8 ± 0.3	24.3 ± 2.5	5.2 ± 0.5	41.3 ± 2.6
vte2 fad2	17.1 ± 2.3	2.8 ± 0.6	0.4 ± 0.1	6.8 ± 1.1	0.5 ± 0.1	25.6 ± 4.5	5.0 ± 0.5	41.9 ± 1.9
fad6	15.9 ± 1.0	10.3 ± 1.0	0 ± 0	0 ± 0	0.3 ± 0.3	30.7 ± 1.6	17.7 ± 0.5	25.1 ± 2.3
vte2 fad6	15.6 ± 0.6	10.3 ± 1.0	0 ± 0	0 ± 0	0.5 ± 0.4	30.5 ± 1.7	*18.6 ± 0.6**	24.5 ± 2.2
fad3	16.1 ± 2.9	3.1 ± 0.4	0.6 ± 0.1	7.0 ± 2.0	0.9 ± 0.1	6.2 ± 1.0	24.7 ± 4.3	41.3 ± 6.4
vte2 fad3	15.1 ± 1.7	3.5 ± 0.7	0.7 ± 0.1	8.0 ± 1.2	0.9 ± 0.1	5.9 ± 0.9	24.3 ± 2.5	41.7 ± 4.0
fad7 fad8	13.2 ± 0.1	2.6 ± 0.1	7.6 ± 0.2	0 ± 0	1.2 ± 0.4	6.2 ± 0.6	55.3 ± 1.7	13.9 ± 1.4
vte2 fad7 fad8	13.0 ± 0.6	2.5 ± 0.2	7.9 ± 0.3	0 ± 0	1.1 ± 0.3	6.6 ± 0.5	55.1 ± 0.6	13.8 ± 1.2
fad3 fad7 fad8	12.4 ± 0.7	2.5 ± 0.1	7.7 ± 1.0	0 ± 0	1.5 ± 0.7	6.4 ± 0.9	69.5 ± 1.3	0 ± 0
vte2 fad3 fad7 fad8	12.4 ± 0.4	2.4 ± 0.1	7.6 ± 0.3	0 ± 0	0.6 ± 0.1	6.1 ± 0.3	70.8 ± 0.5	0 ± 0
After 14 d of LT treatment								
Col	15.9 ± 1.8	1.5 ± 0.1	0.4 ± 0.2	6.4 ± 0.5	1.2 ± 0.8	4.0 ± 0.4	18.2 ± 0.7	52.4 ± 1.8
vte2	17.3 ± 1.4	1.4 ± 0.2	0.4 ± 0.1	6.0 ± 0.7	1.2 ± 0.3	4.1 ± 0.4	*23.7 ± 1.1***	**46.0 ± 2.5****
fad2	23.8 ± 1.7	2.4 ± 0.2	0.3 ± 0.0	3.7 ± 1.2	0.8 ± 0.1	16.8 ± 2.0	13.0 ± 1.3	39.4 ± 3.1
vte2 fad2	**20.4 ± 1.8***	2.3 ± 0.3	**0.2 ± 0.0****	2.4 ± 1.1	0.6 ± 0.2	*24.0 ± 2.2***	13.6 ± 0.9	36.5 ± 4.1
fad6	19.8 ± 0.5	7.5 ± 0.3	0 ± 0	0 ± 0	0.6 ± 0.0	27.3 ± 1.1	22.5 ± 1.2	22.2 ± 1.6
vte2 fad6	19.3 ± 0.6	*8.2 ± 0.3***	0 ± 0	0 ± 0	0.6 ± 0.0	28.0 ± 0.9	*25.1 ± 1.7**	**18.7 ± 1.7***
fad3	16.4 ± 1.0	1.3 ± 0.1	0.2 ± 0.0	6.8 ± 0.5	0.4 ± 0.1	3.2 ± 0.5	28.0 ± 2.4	43.7 ± 3.2
vte2 fad3	*20.5 ± 3.1**	**1.0 ± 0.2***	**0.2 ± 0.0***	**4.6 ± 1.7***	*0.6 ± 0.1**	*4.2 ± 0.7**	31.9 ± 3.0	**37.1 ± 5.2***
fad7 fad8	17.7 ± 0.8	1.7 ± 0.1	5.8 ± 0.5	0 ± 0	0.4 ± 0.0	6.1 ± 0.9	54.1 ± 2.7	14.3 ± 1.9
vte2 fad7 fad8	18.5 ± 0.4	1.5 ± 0.1	5.6 ± 0.1	0 ± 0	*0.5 ± 0.0***	6.1 ± 1.0	*59.9 ± 0.8***	**7.9 ± 0.5****
fad3 fad7 fad8	13.3 ± 0.4	1.5 ± 0.1	6.0 ± 0.4	0 ± 0	0.9 ± 0.4	6.2 ± 0.6	72.1 ± 0.8	0 ± 0
vte2 fad3 fad7 fad8	13.4 ± 0.2	**1.2 ± 0.0****	6.2 ± 0.3	0 ± 0	0.5 ± 0.2	6.1 ± 0.4	72.5 ± 0.6	0 ± 0

Plants were grown at 22°C for 4 weeks and then transferred to 7°C for an additional 14 d. Values are means ± SD ($n = 4$ or 5 biological replicates) from the middle portion of mature leaves and are expressed as mol %. Italics and bold indicate fatty acids that are significantly higher and lower, respectively, in *vte2* or *vte2* containing *fad* mutant lines relative to the corresponding Col, single, or multiple *fad* mutant parents (Student's *t* test, *$P < 0.05$, **$P < 0.01$).

Interestingly, *vte2 fad2*, and to a lesser extent *vte2 fad6*, suppressed the visible phenotype (i.e., purple leaf coloration and reduced plant size) of LT-treated *vte2* (Figure 8A). The suppression of the plant size was even more obvious when 3-week-old plants grown under permissive conditions were transferred to LT (see Supplemental Figure 5 online).

To assess the biochemical consequences of introducing *fad* mutations into the *vte2* background, photoassimilate export capacity and the levels of soluble sugars (i.e., sucrose, glucose, and fructose) were analyzed in all genotypes after 7 and 14 d of LT treatment, respectively. These are the time points when *vte2* and Col first showed differences that were substantial enough to readily detect intermediate levels for these parameters (Maeda et al., 2006). The total soluble sugar content of *fad2*, *fad6*, *fad3*, *fad7 fad8*, and *fad3 fad7 fad8* was similar to Col (29.5 ± 12.3 μmol/gFW) with the exception of a slightly elevated level in *fad3 fad7 fad8* (Figure 9A). The total soluble sugar content of *vte2 fad3*, *vte2 fad7 fad8*, and *vte2 fad3 fad7 fad8* was similar to that of *vte2* (256.6 ± 39.6 μmol/gFW). In *vte2 fad2*, this trait was suppressed to the level in Col, while *vte2 fad6* showed partial suppression and a soluble sugar level intermediate between Col and *vte2* (Figure 9A). The starch levels of *vte2 fad2* and *vte2 fad6* were positively correlated to their sugar levels (see Supplemental Figure 6 online). The photoassimilate export capacity of the different genotypes was negatively correlated to their soluble sugar levels (cf. Figures 9A and 9B). The export capacity of *fad2*, *fad6*, *fad3*, *fad7 fad8*, and *fad3 fad7 fad8* was similar to Col, with the exception of a slightly lower level in *fad3* (Figure 9B). In *vte2*, *vte2 fad3*, *vte2 fad7 fad8*, and *vte2 fad3 fad7 fad8*, we observed similar and dramatically reduced photoassimilate export capacities compared with Col. Interestingly, *vte2 fad2* fully recovered export capacity back to the Col level, while *vte2 fad6* showed significantly higher export capacity than *vte2*, though still lower than Col or *vte2 fad2* (Figure 9B). These results indicate that the introduction of *fad2*, and to a lesser extent *fad6*, but not *fad3*, *fad7 fad8*, or *fad3 fad7 fad8* into the *vte2* background suppresses the impaired photoassimilate export and sugar accumulation phenotypes of *vte2*. The results with *vte2 fad3 fad7 fad8* also indicate that complete elimination of trienoic fatty acids has no impact on the *vte2* LT-induced phenotype.

Having eliminated trienoic fatty acid levels as being involved in induction of the *vte2* LT phenotype, we further analyzed the total fatty acid composition of all genotypes to assess whether one or more other fatty acids might be specifically associated with the *vte2* LT response or its suppression. After 14 d of LT treatment, *vte2* showed reduced 18:3 and increased 18:2 levels relative to Col as expected (Table 1). These LT changes to 18:2 and 18:3 did not occur in the *vte2 fad2* genotype, and instead 18:1 and 16:0

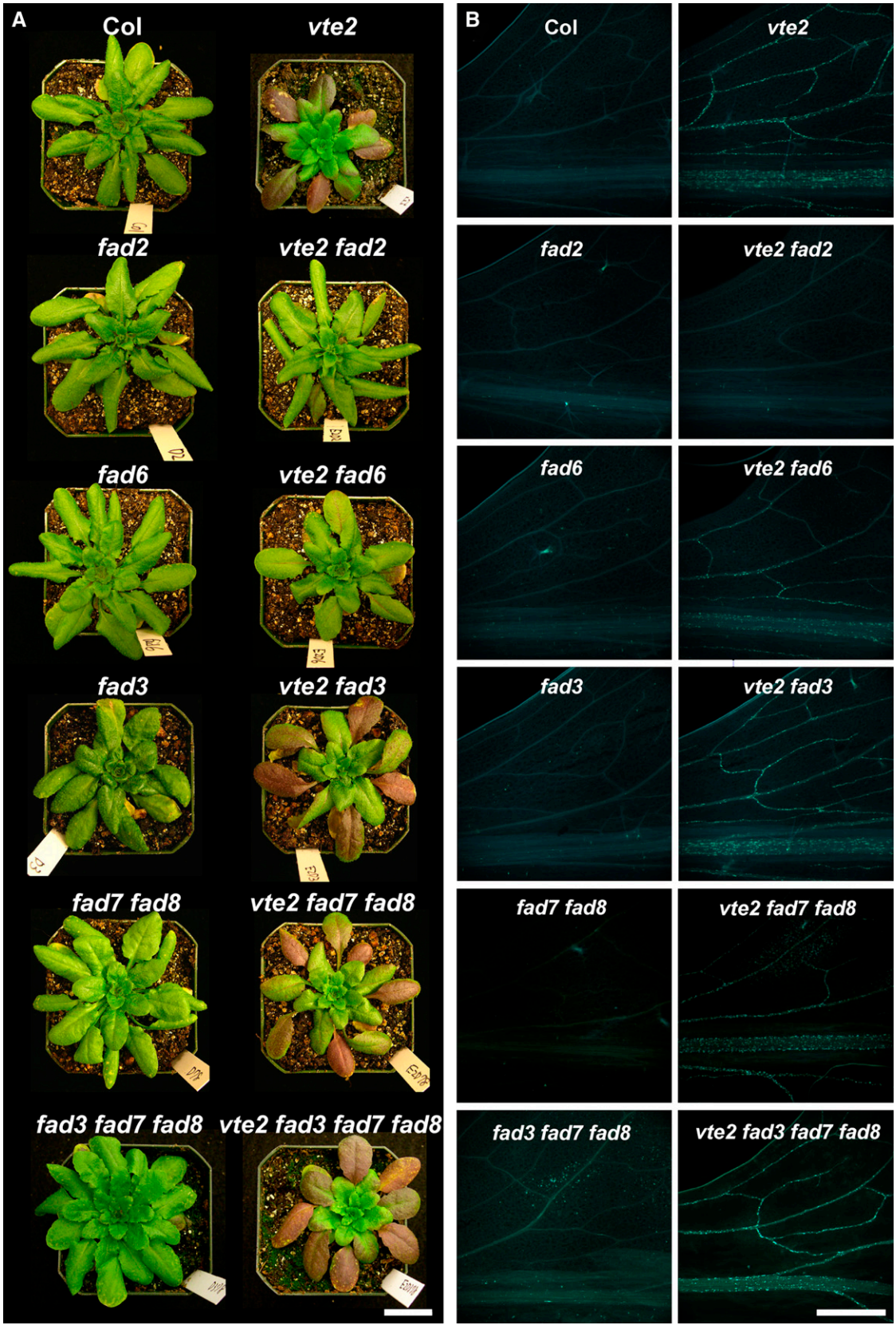

Figure 8. Visible Phenotype and Callose Deposition of LT-Treated Col, *vte2*, and a Series of *fad* and *vte2*-Containing *fad* Mutants.

All genotypes were grown at 22°C for 4 weeks and then transferred to 7°C.
(A) Representative plants of the indicated genotypes after 4 weeks of LT treatment. Bar = 2 cm.
(B) Aniline blue–positive fluorescence in the lower half of the leaves after 3 d of LT treatment. Bar = 1 mm.

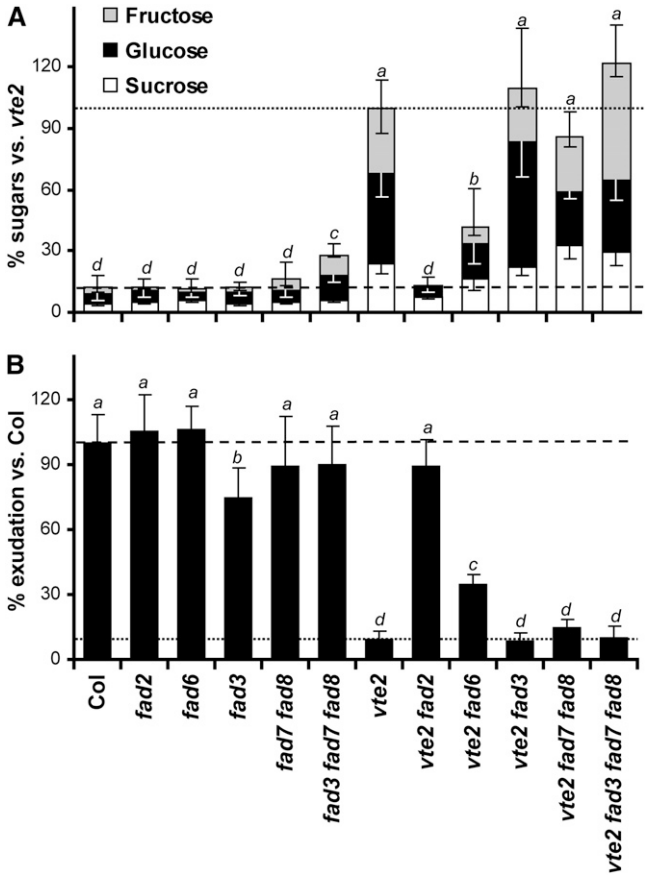

Figure 9. Soluble Sugar Content and Photoassimilate Export Capacity of LT-Treated Col, *vte2*, and a Series of *fad* and *vte2*-Containing *fad* Mutants.

All genotypes were grown at 22°C for 4 weeks and then transferred to 7°C. Nonsignificant groups are indicated by alphabetical order with *a* being the highest (analysis of variance, $P < 0.05$).

(A) After 14 d of LT treatment, mature leaves of the indicated genotypes were harvested at the end of the light cycle and analyzed for total soluble sugar content (i.e., glucose, black; fructose, gray; sucrose, white). Values are means ± SD ($n = 4$ or 5 biological replicates) and expressed as percentage of the *vte2* value (256.6 ± 39.6 μmol/gFW).

(B) After 7 d of LT treatment, mature leaves of the indicated genotypes were labeled with $^{14}CO_2$ in the middle of the day, and ^{14}C-labeled photoassimilate exudation was analyzed as described (Maeda et al., 2006). Data are means ± SD ($n = 5$ or 6 biological replicates) and expressed as percentage of the Col value (18.1% ± 3.1% ^{14}C exudated per total ^{14}C fixed).

were increased and decreased, respectively, in comparison to *fad2*. These 18:2 and 18:3 changes still occurred when *vte2* was present in the *fad3*, *fad6*, and *fad7 fad8* background, with the exception of 18:2 in *vte2 fad3*. These fatty acid changes were almost completely attenuated when *vte2* was present in the *fad3 fad7 fad8* background (Table 1). These results indicate that specific changes in membrane fatty acid composition per se do not correlate with the degree of suppression of the *vte2* LT phenotype in the various *vte2*-containing *fad* mutant genotypes.

fad2 and to a Lesser Extent *fad6* Suppress the Abnormal Transfer Cell Wall Development of LT-Treated *vte2*

Previous studies have demonstrated that reductions in photoassimilate export in LT-treated *vte2* coincide with abnormal cell wall morphology and callose deposition exclusively in phloem parenchyma transfer cells (Maeda et al., 2006). To test if introduction of the *fad* mutations into the *vte2* background also affects the vascular specific callose deposition at LT, 0-, 3-, and 7-d LT-treated plants were harvested and aniline blue–positive fluorescence was analyzed as a marker of callose deposition. The vascular tissue of Col and all *fad* mutants (*fad2*, *fad6*, *fad3*, *fad7 fad8*, and *fad3 fad7 fad8*) lacked aniline blue–positive fluorescence at all time points (Figure 8B; see Supplemental Figure 7 online). By contrast, vascular specific aniline blue–positive fluorescence appeared at the base of *vte2* leaves at 3 d and spread through the entire leaf by 7 d (Figure 8B; see Supplemental Figure 7 online; Maeda et al., 2006). *vte2 fad3*, *vte2 fad7 fad8*, and *vte2 fad3 fad7 fad8* showed the same patterns of aniline blue–positive fluorescence as *vte2. vte2 fad6* also showed similar patterns to *vte2*, though the development and degree of fluorescence in *vte2 fad6* was slightly slower and lower, respectively, than *vte2* at 3 d (Figure 8B) but not at 7 d (see Supplemental Figure 7 online). *vte2 fad2* had a background level of fluorescence at all time points (Figure 8B; see Supplemental Figure 7 online). These results indicate that *fad2* and to a much lesser extent *fad6* but not *fad3*, *fad7 fad8*, or *fad3 fad7 fad8* suppress the vascular specific callose deposition observed in LT-treated *vte2*.

We further compared the patterns of phloem parenchyma transfer cell wall development and callose deposition among LT-treated Col, *vte2*, and *vte2 fad2* and *vte2 fad6*, the two *vte2*-containing *fad* lines that suppressed the photoassimilate export and callose deposition phenotypes of *vte2*. Paradermal serial sections and cross sections were examined with the transmission electron microscope after 3 d of LT treatment. In Col, nascent, papillate cell wall ingrowths commonly found in other species (DeWitt et al., 1999; Schmidt et al., 2000; Talbot et al., 2001, 2002, 2007; Offler et al., 2002; Vaughn et al., 2007) were initiated along the primary wall and were spatially associated with Golgi, ER, and endomembrane vesicles (Figure 10A). Transfer cell wall maturation progressed as described by Talbot et al. (2001); papillate cell wall ingrowths branched (Figure 10B) and coalesced (Figure 10C) to form a base upon which more papillate projections were initiated (Figure 10D) that also branched and fused to subsequently give rise to a mature fenestrated cell wall that was composed of both an electron-opaque inner region and electron-translucent outer region (Figures 10E and 10F), typical of transfer cell wall structure (Vaughn et al., 2007). The LT-induced initiation and maturation of transfer cell walls in *fad2* and *fad6* were similar to Col (see Supplemental Figure 8 online).

The initiation of transfer cell wall development in *vte2* and *vte2 fad6* was also similar to Col as indicated by the presence of papillate cell wall ingrowths (Figure 11A; see Supplemental Figure 8 online) that branched laterally (Figure 11B) and fused (Figure 11C). However, unlike Col, developmental polarity was absent in *vte2*, and papillae were initiated around the entire cell. Further maturation of the transfer cell wall in *vte2* ensued with the

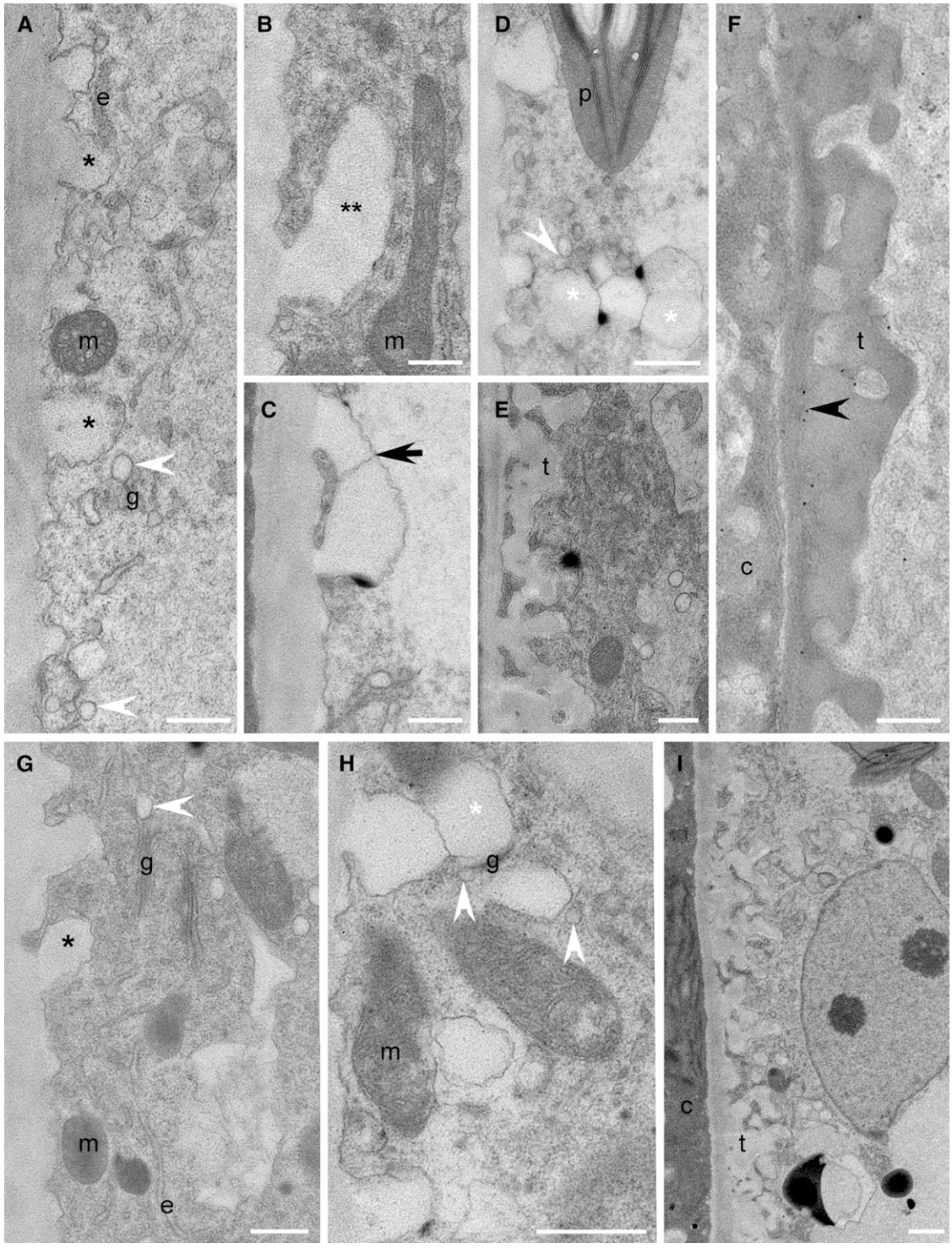

Figure 10. Cellular Structure, Cell Wall Development, and Immunodetection of β-1,3-Glucan in Col and *vte2 fad2* after 3 d of LT Treatment.

(A) to **(F)** Col.

(G) to **(I)** *vte2 fad2*.

(A) to **(I)** Immunodetection of β-1,3-glucan. Single black asterisks mark nascent transfer cell wall papillae (**[A]** and **[G]**). Double asterisks mark laterally elongating nascent papillate ingrowth **(B)**. Black arrow marks fused, elongated papillae **(C)**. White asterisks mark spherical wall ingrowths that have developed on preexisting wall ingrowths (**[D]** and **[H]**). White arrowheads mark Golgi-derived vesicles (**[A]**, **[D]**, **[G]**, and **[H]**). Black arrowhead marks positive immunodetection of β-1,3-glucan **(F)**. c, companion cell; e, endoplasmic reticulum; g, Golgi; m, mitochondrion; p, plastid, t, transfer cell wall. Bars = 0.5 μm.

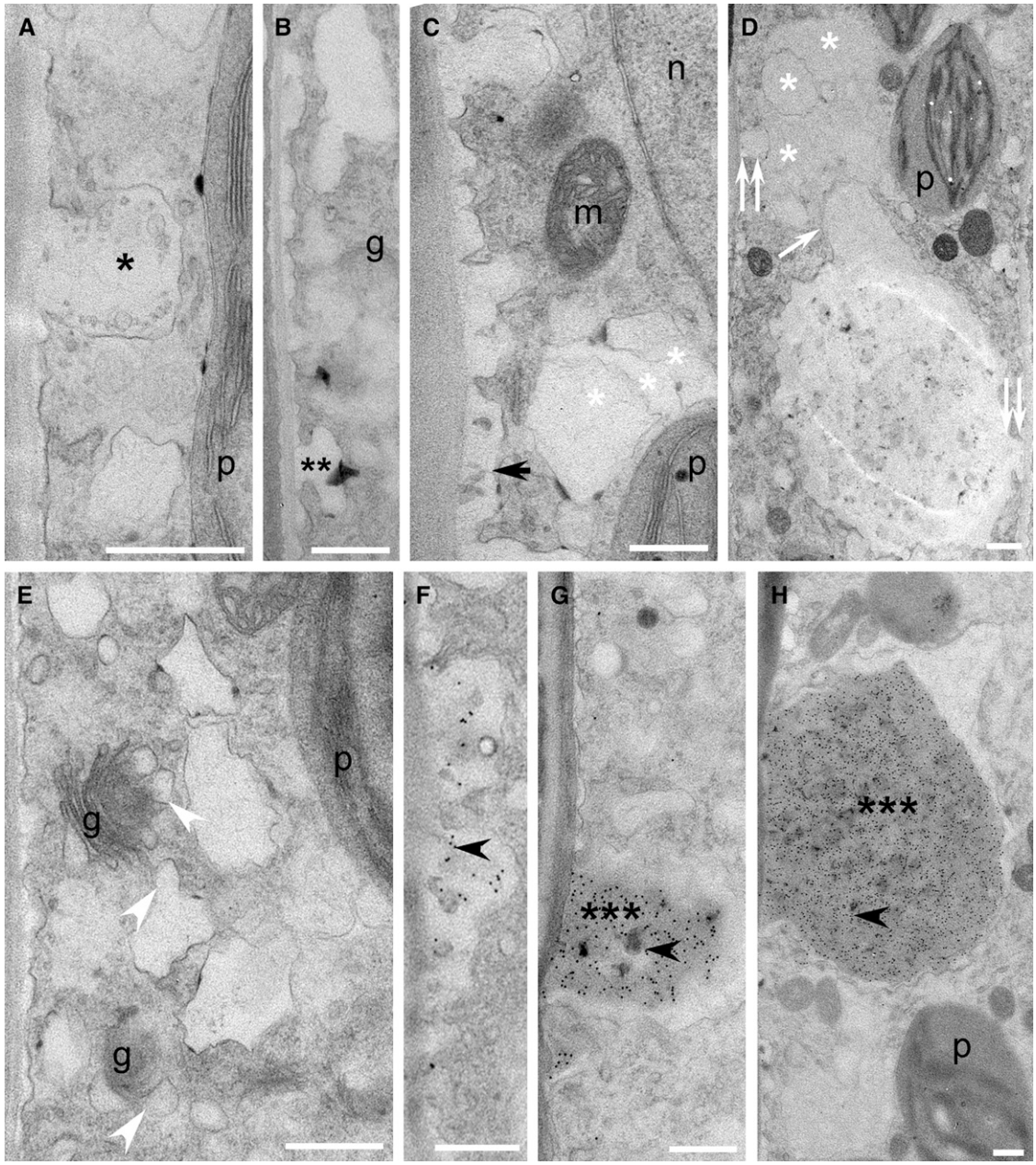

Figure 11. Cellular Structure, Cell Wall Development, and Immunodetection of β-1,3-Glucan in *vte2* after 3 d of LT Treatment.

(A) to **(H)** *vte2*. g, Golgi; m, mitochondrion; n, nucleus; p, plastid. Bars = 0.5 μm.
(A) and **(F)** to **(H)** Immunodetection of β-1,3-glucan.
(A) Single black asterisk marks nascent transfer cell wall papilla.
(B) Double asterisks label laterally elongating nascent papillate ingrowth.
(C) Black arrow marks fused, elongated papillae.
(C) and **(D)** White asterisks mark hypertrophied, deformed wall ingrowths that have developed on preexisting wall ingrowths during early **(C)** and later stages **(D)** of development.
(D) White arrow marks two coalesced ingrowths with origins on opposite sides of the cell as indicated by double white arrowheads.
(E) White arrowheads mark swollen, misshapen Golgi-derived vesicles.
(F) to **(H)** Black arrowheads mark positive immunodetection of β-1,3-glucan following fusion of laterally elongated papilla **(F)**, through to the development of continuously enlarging tumor-like ingrowths marked by triple black asterisks (**[G]** and **[H]**).

continuous development of hypertrophied, deformed ingrowths on the preexisting ingrowths (Figure 11C) that subsequently coalesced and occluded the cell (Figure 11D). Golgi-derived vesicles associated with developing wall ingrowths of LT-treated *vte2* were noticeably swollen and misshapen (Figure 11E) compared with those of Col (Figures 10A and 10D). In LT-treated *vte2 fad6*, developing ingrowths were varied in structure and were either unevenly thickened and lacking extensive branching, grossly enlarged, or in some cases normal (see Supplemental Figure 8 online). Interestingly, in *vte2 fad2*, both initiation and development of transfer cell walls were completely normal and proceeded as in Col (Figures 10G to 10I).

The nascent papillae of all LT-treated genotypes lacked epitopes recognized by monoclonal antibodies to β-1,3-glucan (Figures 10A, 10G, and 11A; see Supplemental Figure 8 online). Positive immunolocalization for β-1,3-glucan was absent (Figures 10E and 10I) to low (Figure 10F) in LT-treated Col and *vte2 fad2* and, when present, was only observed at the later stages of transfer cell wall maturation (Figure 10F). By contrast, in *vte2*, positive immunolocalization for β-1,3-glucan was noted continuously following the time of convergence of laterally elongated papillae (Figure 11F) through to the development of tumor-like ingrowths (Figures 11G and 11H). These observations indicate that the *vte2* mutant appears to have normal initiation of LT-induced transfer cell walls but that their development and maturation is abnormal, a process that is completely and partially suppressed by introduction of the *fad2* and *fad6* mutations, respectively.

DISCUSSION

All plants produce and accumulate tocopherols, yet their functions are only beginning to be understood in photosynthetic organisms. Previous studies revealed that tocopherols play a crucial role in phloem loading and carbohydrate metabolism in maize, potato, and cold-treated *Arabidopsis* (Russin et al., 1996; Provencher et al., 2001; Porfirova et al., 2002; Sattler et al., 2003; Hofius et al., 2004; Maeda et al., 2006). Tocopherol-deficient mutants of *Arabidopsis* exhibit abnormal development of phloem parenchyma transfer cell walls and inhibited photoassimilate export as early as 6 h after LT treatment, and this is followed by elevated carbohydrate accumulation and ultimately growth inhibition (Maeda et al., 2006). Although these phenotypes were shown to be independent of any photoprotective role of tocopherols, the underlying mechanisms were unknown. This study focused on the impacts of tocopherol deficiency on membrane structure and dynamics in LT-treated *Arabidopsis* leaves to further understand tocopherol functions at LT.

Prior to LT treatment, the fatty acid and lipid composition of *vte2* and the wild type were indistinguishable, with the exception of petiole tissue. In response to LT treatment, *vte2* (and *vte1*, a second tocopherol-deficient locus; Sattler et al., 2003) showed higher 18:2 and lower 18:3 levels than the wild type (Figure 1; data not shown). Consistent with a prior study reporting no detectable increase in lipid peroxides in LT-treated *vte2* (Maeda et al., 2006), MS-based analysis for lipids with oxidized 18-carbon acyl chains showed that almost all were at low levels and not significantly different between LT-treated *vte2* and the wild type (Figure 4). Analysis of jasmonic acid (JA), OPDA, and phytoprostanes, all 18:3-derived oxylipins (Howe and Schilmiller, 2002; Farmer et al., 2003; Mueller, 2004), also showed no obvious increase in LT-treated *vte2* (see Supplemental Figure 9 online). These combined data indicate that enhanced 18:3 oxidation does not contribute to the reduction in 18:3 levels in LT-treated *vte2* relative to the wild type.

Given that the majority of tocopherols reside in plastids, we anticipated that the 18:3 reduction in *vte2* would occur primarily in PUFAs and lipids derived from the chloroplast pathway. However, lipidomics showed that the level of plastid-derived 18:3-containing lipid species were indistinguishable between genotypes in 3-d LT-treated petioles and was higher rather than lower in *vte2* relative to the wild type after 14 d of LT treatment. By contrast, 18:3-containing species derived from the ER pathway were significantly reduced, and ER-derived 18:2-containing species were correspondingly increased in 3-d LT-treated petioles (Figure 3B). These differences were persistent and further exaggerated in 14-d LT-treated *vte2*. Although some ER pathway–derived 18:3-containing lipid species (e.g., 18:3-18:3 of PC) are imported back into the chloroplast and could eventually affect chloroplast membrane composition (Figure 3C; Roughan et al., 1980; Browse et al., 1986b), the results clearly indicate that tocopherol deficiency preferentially impacts ER, rather than chloroplastic, lipid metabolism. The results from [^{14}C]-acetate labeling analysis during the initial 8 d of LT treatment are in good agreement with steady state lipidomic analysis: less and more ^{14}C label was incorporated into newly synthesized trienoic and dienoic fatty acids, respectively, in *vte2* relative to the wild type at LT (Figure 5A), and these differences occur primarily in fatty acids esterified to ER-synthesized PC and PE but not chloroplast-synthesized MGDG (Figure 6; see Supplemental Figure 2 online). Finally, the fatty acid turnover rate was similar between LT-treated *vte2* and the wild type (Figure 7). These combined results allow us to conclude that the primary impact of tocopherol deficiency on lipids at LT is not on oxidation or metabolism of PUFAs in the chloroplast but rather on the conversion of dienoic to trienoic fatty acids in lipids produced in the ER.

Genetic modification of plastidic or extraplastidic PUFA synthesis by the introduction of a series of *fad* mutations into the *vte2* background not only supports this conclusion but also provides further insights into the underlying mechanisms of the *vte2* LT-induced phenotypes. The disruption of trienoic fatty acid synthesis in the ER or plastid pathways (i.e., in *vte2 fad3* and *vte2 fad7 fad8*) or the complete elimination of trienoic fatty acid synthesis in both compartments (i.e., in *vte2 fad3 fad7 fad8*) had no impact on the LT-induced phenotypes of *vte2* (Figures 8 and 9). This was in sharp contrast with the full suppression of the *vte2* seedling phenotype in *vte2 fad3 fad7 fad8* (Mène-Saffrané et al., 2007). Although it has been speculated that tocopherols are involved in the regulation of trienoic fatty acid–derived signals (Munne-Bosch and Falk, 2004, 2007), these data conclusively eliminate the possibility that such compounds (e.g., JA, OPDA, dinor-OPDA, and phytoprostanes) play a role in the initiation or development of the tocopherol-deficient *vte2* LT phenotype. Furthermore, because trienoic fatty acids (i.e., 18:3 and 16:3) make up ~95% of the PUFAs esterified to MGDG and DGDG, the most abundant lipids in the chloroplast (Browse et al., 1989;

Miquel and Browse, 1992), these genetic data together with the delayed and relatively minor impact of *vte2* on galactolipid species during LT treatment (Figure 3B) indicate that changes to galactolipids are not responsible for the *vte2* LT phenotype. In contrast with *fad3*, *fad7*, and *fad8*, the introduction of *fad2* or *fad6*, mutations that affect the conversion of monoenoic to dienoic fatty acids in the ER and chloroplast, respectively, had dramatic impacts on the *vte2* LT-induced phenotypes: *fad2* completely suppressed while *fad6* partially suppressed nearly all *vte2* LT phenotypes (Figures 8 to 11; see Supplemental Figures 5 to 8 online). Because *fad2* and to a lesser extent *fad6* primarily affect the fatty acid composition of phospholipids (Browse et al., 1989; Miquel and Browse, 1992), alterations in phospholipid acyl chains by *fad2* or *fad6* mutations are likely involved in the suppression of the *vte2* LT phenotype, consistent with the rapid and major impact of *vte2* on phospholipid molecular species during LT treatment (Figure 3B). These combined results provide genetic and biochemical evidence that membrane lipid metabolism, especially ER lipid metabolism, plays a central role in the *vte2*-dependent LT-induced phenotypes.

Extraplastidic Functions of Tocopherols in Plants

Because tocopherols are synthesized in plastids (Soll et al., 1980, 1985; DellaPenna and Pogson, 2006), they have long been assumed to have essential functions restricted to this organelle (Fryer, 1992; Munne-Bosch and Alegre, 2002). However, recent studies using tocopherol-deficient photosynthetic organisms have brought such an assumption into question (Maeda and DellaPenna, 2007). Tocopherol deficiency in *Arabidopsis* and *Synechocystis* sp PCC6803 has surprisingly subtle impacts on responses to high intensity light stress, which primarily causes oxidative stress in the chloroplast (Dahnhardt et al., 2002; Porfirova et al., 2002; Havaux et al., 2005; Maeda et al., 2005, 2006). Several studies suggested that tocopherol deficiency may be partially compensated for by other antioxidants (e.g., carotenoids) during high light stress (Havaux et al., 2005; Maeda et al., 2005, 2006). By contrast, evidence has been accumulating suggesting that tocopherol deficiency impacts specific extraplastidic processes. Using the *Arabidopsis vte2* mutants, Sattler et al. (2004, 2006) have shown that tocopherols are essential in preventing oxidation of PUFAs in triacylglycerols in seed oil bodies, organelles derived from the ER in which up to 40% of seed tocopherols accumulate (Yamauchi and Matsushita, 1976; Fisk et al., 2006; White et al., 2006). Transfer cell wall development at the plasma membrane is also severely impacted during LT treatment of *Arabidopsis vte2* (Maeda et al., 2006) as is plasmodesmatal structure in the maize tocopherol-deficient *sxd1* mutant (Russin et al., 1996; Provencher et al., 2001), which is coincident with impaired photoassimilate export in both systems. Data from this study are consistent with the hypothesis that tocopherols have an extraplastidic function in ER lipid metabolism that causes abnormal transfer cell wall development and impaired photoassimilate export during LT adaptation of *Arabidopsis*. The impaired photoassimilate export phenotype of other tocopherol-deficient mutants, such as maize and potato *sxd1* (Russin et al., 1996; Provencher et al., 2001; Hofius et al., 2004), may also be associated with similar changes in ER lipid metabolism. Introducing the orthologous *fad2* and *fad6* mutations into tocopherol-deficient maize or potato *sxd1* backgrounds could directly test this hypothesis.

How do plastid-synthesized tocopherols affect lipid metabolism in extraplastidic membranes? It has been well documented that fatty acids produced in the chloroplast are exported to the ER and transported back to the chloroplast (Browse et al., 1986b; Pollard and Ohlrogge, 1999). Recently, the ER membrane was demonstrated to have plastid-associated membranes (Andersson et al., 2006) that provide a physical connection between the chloroplast envelope and ER membranes and could allow transfer of lipids and tocopherols between these two compartments. Given that tocopherols are synthesized in the chloroplast inner envelope (Soll et al., 1980, 1985) but are equally abundant in the inner and outer envelope membranes (Soll et al., 1985), outer envelope-localized tocopherols may also be transported to extraplastidic membranes or at least preferentially localize to the plastid-associated membrane regions where they could directly interact with and impact the ER membrane or enzymes involved in ER PUFA and lipid metabolism. However, at this point, we cannot exclude the possibility that other chloroplast-derived molecules might also impact ER lipid metabolism as well.

While it is clear that alteration of ER-derived phospholipids is a direct result of the tocopherol deficiency in LT-treated *vte2*, it is less clear how this leads to aberrant transfer cell wall development. Transfer cells develop primarily at boundaries between the symplast and apoplast (Offler et al., 2002), and LT strongly stimulates phloem parenchyma transfer cell wall development in *Arabidopsis* (Figure 10) presumably to increase the plasma membrane surface area and associated transporters to maintain photoassimilate transport capacity at LT (Bonnemain et al., 1991; Harrington et al., 1997; Weber et al., 1997; Bagnall et al., 2000). The magnitude and rapidity of transfer cell wall development at LT in *Arabidopsis* places an extreme demand on the secretory endomembrane system and extraplastidic lipid metabolism for deposition and maintenance of cell wall and plasma membranes (Offler et al., 2002). Indeed, we found that high levels of endomembrane system components (i.e., ER, Golgi, and associated vesicles) permeate *Arabidopsis* phloem parenchyma transfer cells (Figures 10 and 11). In LT-treated *vte2*, initiation of wall papilla appears to occur normally (Figure 11A), but polarized transfer cell wall maturation is disrupted (Figures 11D and 11E), leading to distorted wall ingrowths that become grossly amplified and accumulate callose (Figures 11G and 11H; Maeda et al., 2006). Interestingly, the abnormal cell wall maturation in LT-treated *vte2* is associated with hypertrophied Golgi-derived vesicles that appear to be involved in deposition of transfer cell wall components (Figures 11B and 11E; Aubert et al., 1996). Studies in animal systems have shown that in addition to regulating vesicular, organellar, and cellular membrane biogenesis and morphology, specific membrane PUFAs modulate vesicle fusion primarily through their interactions with SNAREs, key proteins for membrane trafficking in all eukaryotes including plants (Darios and Davletov, 2006; Connell et al., 2007; Davletov et al., 2007; Latham et al., 2007).

Based on our observation and these animal studies, we hypothesize that alteration in extraplastidic lipid metabolism as a result of tocopherol deficiency affects properties of Golgi-derived

vesicles, thereby disrupting secretory processes that function in normal transfer cell wall maturation in *Arabidopsis* at LT. The LT-induced transfer cell wall development of *Arabidopsis* phloem parenchyma cells and the maturation phase-specific defect observed in *vte2* provide a model system to further dissect the control of transfer cell wall deposition and the underlying mechanism of the extraplastidic functions of tocopherols in plants.

METHODS

Plant Materials and Construction of Double and Triple Homozygous Lines

The *fad2-1*, *fad3-2*, *fad6-1*, and *fad7-1 fad8-1* mutants were obtained from the ABRC. The *vte2-1* mutant has been previously isolated and backcrossed three times (Sattler et al., 2004). All genotypes are in the Col background. The *vte2-1 fad2-1*, *vte2-1 fad3-2*, *vte2-1 fad6-1* double, *vte2-1 fad7-1 fad8-1* triple, and *vte2-1 fad3-2 fad7-2 fad8-1* quadruple mutants were selected from crosses of the respective single or double mutant parents. F2 progeny homozygous for the *vte2-1* mutation were identified by HPLC based on their tocopherol deficiency (Sattler et al., 2004) and confirmed by genotyping with a *vte2-1* cleaved-amplified polymorphic sequence marker, 5′-TTTCACTGGCATCTTGGAGGTA-ATG-3′ and 5′-AAGTGGCAACTGTTTGTAGTAGAAG-3′, which generates a 632-bp PCR product with a *Sac*I site for the *vte2-1* allele. F2 progeny homozygous for the respective *fad* mutation were identified by fatty acid methyl ester analysis using gas–liquid chromatography as described previously (Browse et al., 1986a).

Growth Conditions and LT Treatment

Seeds were stratified for 4 to 7 d (4°C), planted in an equal mixture of vermiculite, perlite, and soil fertilized with 1× Hoagland solution (see Supplemental Methods 1 online), and grown in a chamber under permissive conditions: 12 h, 120 μmol photon m^{-2} s^{-1} light at 22°C/12 h darkness at 18°C with 70% relative humidity. Plants were watered every other day and with 0.5× Hoagland solution once a week. For LT treatments, 3- to 4-week-old plants were transferred at the beginning of the light cycle to 12 h 75 μmol photon m^{-2} s^{-1} light/12 h darkness at 7°C (±<3°C).

Carbohydrate Analyses, Phloem Exudation Experiments, and Callose Detection

Leaf-soluble sugar content (i.e., glucose, fructose, and sucrose) was quantified using an enzymatic assay previously described (Maeda et al., 2006). Phloem exudation experiments were conducted according to Maeda et al. (2006) except that 0.05 mCi of $NaH^{14}CO_3$ were converted to $^{14}CO_2$ for each labeling experiment and 10 mM EDTA was used for exudation buffer. Phloem exudates were collected after 5 h of exudation. The photoassimilate export capacity was measured as a percentage of radioactivity exudated per total radioactivity fixed. Callose deposition was visualized by aniline blue–positive fluorescence as previously described (Maeda et al., 2006).

Lipid Profiling

The profiles of individual lipid molecular species were obtained by an automated electrospray ionization tandem mass spectrometry approach as described previously (Devaiah et al., 2006). The 7th to 10th oldest leaves from 4-week-old plants grown under permissive conditions were cold treated for the indicated time, collected, and immediately immersed in 75°C isopropanol containing 0.01% butylated hydroxytoluene (BHT). Total lipids were extracted as described by Welti et al. (2002) and dissolved in chloroform for analysis.

Oxidized Lipid Analysis

Based on Q-TOF analysis, the acyl anions corresponding to 18-carbon oxylipins, $C_{18}H_{27}O_3$ (mass-to-charge ratio [*m/z*] 291), $C_{18}H_{29}O_3$ (*m/z* 293), and $C_{18}H_{31}O_3$ (*m/z* 295), were designated as 18:4-O, 18:3-O, and 18:2-O species, respectively, with the abbreviations indicating the number of carbon atoms, the number of double bond equivalents that include C=C, C=O, or ring formation and the number of oxygen atoms in addition to the carbonyl oxygen (Buseman et al., 2006). Furthermore, the Q-TOF analysis indicated that these oxidized species, 18:4-O, 18:3-O, and 18:2-O, are the major and generally the only lipid fragments with nominal *m/z* of 291, 293, and 295 (Buseman et al., 2006; Esch et al., 2007). The level of oxylipin-containing lipid molecular species was quantified by precursor scanning of oxylipin acyl anions, *m/z* 291, 293, and 295, using a triple quadrupole mass spectrometer (API 4000; Applied Biosystems) in the negative mode. The lipid extracts from 3-d LT-treated petioles were dissolved in chloroform/methanol/aqueous 300 mM ammonium acetate (NH_4OAc) and used for the analysis. PE and PG species were identified as $[M - H]^-$, PC species were identified as $[M + OAc]^-$, and MGDG and DGDG species were identified as either $[M - H]^-$ or as $[M + OAc]^-$ (see Supplemental Figure 1 online). Product (Q-TOF) and precursor (triple quadrupole) scanning demonstrated that product ion fragments correspond either to entire acyl anions or to an acyl anion that has lost a water molecule during collision-induced dissociation; i.e., in some cases, *m/z* 291 and 293 species have undergone a loss of water from *m/z* 309, $C_{18}H_{29}O_4$ (18:3-2O) and *m/z* 311, $C_{18}H_{31}O_4$ (18:2-2O), respectively (see Supplemental Figure 1 online). Although it is conceivable that oxylipins of higher masses could produce *m/z* 291, 293, or 295 fragments through additional water losses, examination of the detected precursor ion species indicated that pairing *m/z* 291, 293, 295, 309, and 311 with common and expected acyl species accounted for most of the spectral peaks observed (see Supplemental Figure 1 online). Baselines were subtracted, data were smoothed, and the centroids of a mass spectral peak were determined (Analyst software; Applied Biosystems; for spectral display only, peak intensities within one mass unit were binned). For quantification, peak intensities were corrected for isotopic overlap from nearby peaks. Mass spectral signals were normalized to the signal for 230 pmol di24:1 PG, an unnaturally occurring lipid species that was added to the portion of the sample being analyzed as an internal standard; relative mass spectral signal/dry weight was calculated as the following equation:

$$\frac{\text{mass spectral signal for indicated species} \times 230}{\text{mass spectral signal for di24 : 1 PG} \times \text{fraction of sample analyzed} \times \text{dry weight}}$$

Although no corrections for varying mass spectral response to the various molecular species have been applied, these data provide for direct comparison of the relative amounts of each molecular species in wild-type plants compared with mutant plants.

Lipid Labeling Experiments

The 7th to 10th oldest leaves from 4-week-old plants grown under permissive conditions were labeled with 10 μL of 50 μCi/mL sodium [1-^{14}C]-acetate by applying 0.5 to 1 μL droplets to the leaf surface (Browse et al., 1986b; Xu et al., 2003). Four labeled leaves were harvested into liquid nitrogen from two plants after 2, 24, 72, 120, and 192 h of labeling. $^{14}CO_2$ pulse labeling experiments were conducted in a tightly sealed 10-liter glass chamber as described (Maeda et al., 2006) using 2- to 3-week-old plants and 0.5 mCi of $NaH^{14}CO_3$ for acid-catalyzed production of $^{14}CO_2$.

Total lipids were extracted in hot isopropanol as described (Hara and Radin, 1978) and separated on 0.15 M ammonium sulfate-impregnated TLC plates (Whatman K6 silica gel 60 Å) using 91/30/8 (v/v/v) acetone/toluene/water with 0.01% BHT as a solvent system. The TLC plates were sprayed with 0.1% dichlorofluorescein (Sigma-Aldrich) to locate individual band locations under UV light, and the MGDG, PC, and PE bands were recovered and directly used for transesterification using 1 N hydrochloric acid-methanol (Supelco; Browse et al., 1986a). The resulting fatty acid methyl esters were separated based on the numbers of double bonds by argentation (silver-coated) TLC (Morris, 1966). TLC plates were impregnated with 10% (w/v) $AgNO_3$ in acetonitrile, activated for 5 min at 100°C, developed three quarters of the way in 50% (v/v) and fully in 10% (v/v) diethyl ether in hexane with 0.01% BHT. The radioactivity in each band was quantified by exposing the plates to a phosphor screen together with standards with known radioactivity (Storm; GE Healthcare). Because the 30-min labeling time with $^{14}CO_2$ will not saturate the lipid pool with ^{14}C, the rate of fatty acid turnover calculated may be underestimated.

Transmission Electron Microscopy

Leaves were harvested in the middle of the third day after transfer to LT (54 h of LT treatment) and prepared for transmission electron microscopy and immunolocalization of β-1,3-glucan as described by Maeda et al. (2006).

Accession Numbers

Sequence data from this article can be found in the Arabidopsis Genome Initiative or GenBank/EMBL databases under the following accession numbers: *Arabidopsis Vte1* (At4g32770/AF302188), *Vte2* (At2g18950/AF324344), *Fad2* (At3g12120/NM112047), *Fad3* (At2g29980/NM128552), *Fad6* (At4g30950/NM119243), *Fad7* (At3g11170/NM111953), and *Fad8* (At5g05580/NM120640). Seed information for the *Arabidopsis* mutants used in this study can be found in The Arabidopsis Information Resource: *fad2-1* (CS8041), *fad3-2* (CS8034), *fad6-1* (CS207), and *fad7-1 fad8-1* (CS8036). Seeds of double, triple, and quadruple mutants in the *vte2* background do not germinate after a few months of storage (see Sattler et al., 2004) and thus are maintained in the authors' lab and are available upon request.

Supplemental Data

The following materials are available in the online version of this article.

Supplemental Figure 1. Individual Oxylipin-Containing Lipid Species Analyzed in Figure 4.

Supplemental Figure 2. Redistribution of Radioactivity among the Fatty Acids of Total Lipids or Individual Lipids of LT-Treated Col and *vte2*.

Supplemental Figure 3. $^{14}CO_2$ Pulse Chase Labeling of Total Fatty Acids in LT-Treated Col and *vte2*.

Supplemental Figure 4. Visible Phenotype before LT Treatment of Col, *vte2*, and a Series of *fad* and *vte2*-Containing *fad* Mutants.

Supplemental Figure 5. Visible Phenotype of LT-Treated Col, *vte2*, *fad2*, *fad6*, *vte2 fad2*, and *vte2 fad6*.

Supplemental Figure 6. Starch Content of LT-Treated Col, *vte2*, *fad2*, *fad6*, *vte2 fad2*, and *vte2 fad6*.

Supplemental Figure 7. Callose Deposition of Col, *vte2*, and a Series of *fad* and *vte2*-Containing *fad* Mutants after Prolonged LT Treatment.

Supplemental Figure 8. Cellular Structure, Cell Wall Development, and Immunodetection of β-1,3-Glucan in *fad2*, *fad6*, and *vte2 fad6* after 3 d of LT Treatment.

Supplemental Figure 9. The Level of JA, OPDA, and Phytoprostane in Col and *vte2-1* during LT Treatment.

Supplemental Table 1. Fatty Acid Composition of Total Lipid Extracts from *vte2* and Col Leaves and Petioles during a 14-d Time Course of LT Treatment.

Supplemental Methods 1. The Composition of the Hoagland Solution Used in This Study.

ACKNOWLEDGMENTS

We thank Kathy Sault for technical assistance with microscopy, John Ohlrogge and Philip Bates for advice in labeled lipid analyses, Edward E. Farmer and Laurent Mène-Saffrané for the *vte2 fad3 fad7 fad8* quadruple mutant, Scott Sattler for the *vte2 fad3* double mutant, William Pasutti for assistance in selection of the *vte2 fad6* double mutant, Ethan Baughman, Pamela Tamura, and Mary Roth for Q-TOF analysis of *Arabidopsis* lipid species, Martin Mueller for phytoprostane analysis, and members of the DellaPenna lab for their critical advice, discussions, and manuscript review. The Kansas Lipidomics Research Center Analytical Laboratory was supported by grants from the National Science Foundation (MCB-0455318 and DBI-0521587) and the National Science Foundation's Experimental Program to Stimulate Competitive Research (EPS-0236913), with matching support from the state of Kansas through Kansas Technology Enterprise Corporation and Kansas State University, as well as from National Institutes of Health Grant P20 RR016475 from the IDeA Network of Biomedical Research Excellence program of the National Center for Research Resources. This work was supported by a Michigan State University strategic partnership grant and National Science Foundation Grant MCB-023529 to D.D. and a Connaught Award and Natural Sciences and Engineering Research Council of Canada Discovery Grant to T.L.S.

Received July 31, 2007; revised January 4, 2008; accepted February 9, 2008; published February 26, 2008.

REFERENCES

Andersson, M.X., Goksor, M., and Sandelius, A.S. (2006). Optical manipulation reveals strong attracting forces at membrane contact sites between endoplasmic reticulum and chloroplasts. J. Biol. Chem. **282:** 1170–1174.

Aubert, S., Gout, E., Bligny, R., Marty-Mazars, D., Barrieu, F., Alabouvette, J., Marty, F., and Douce, R. (1996). Ultrastructural and biochemical characterization of autophagy in higher plant cells subjected to carbon deprivation: control by the supply of mitochondria with respiratory substrates. J. Cell Biol. **133:** 1251–1263.

Bagnall, N., Wang, X.D., Scofield, G.N., Furbank, R.T., Offler, C.E., and Patrick, J.W. (2000). Sucrose transport-related genes are expressed in both maternal and filial tissues of developing wheat grains. Aust. J. Plant Physiol. **27:** 1009–1020.

Bonaventure, G., Ba, X.M., Ohlrogge, J., and Pollard, M. (2004). Metabolic responses to the reduction in palmitate caused by disruption of the FATB gene in *Arabidopsis.* Plant Physiol. **135:** 1269–1279.

Bonnemain, J.L., Borguin, S., Renault, S., Offler, C.E., and Fincher, G.B. (1991). Transfer cells: Structure and physiology. In Recent Advances in Phloem Transport and Assimilate Compartmentation, L. Bonnemain and S. Delrot, eds (Paris: Presses Académiques), pp. 74–83.

Blée, E., and Joyard, J. (1996). Envelope membranes from spinach chloroplasts are a site of metabolism of fatty acid hydroperoxides. Plant Physiol. **110:** 445–454.

Bramley, P.M., Elmadfa, I., Kafatos, A., Kelly, F.J., Manios, Y., Roxborough, H.E., Schuch, W., Sheehy, P.J.A., and Wagner, K.H. (2000). Vitamin E. J. Sci. Food Agric. **80:** 913–938.

Browse, J., Kunst, L., Anderson, S., Hugly, S., and Somerville, C. (1989). A mutant of *Arabidopsis* deficient in the chloroplast 16-1/18-1 desaturase. Plant Physiol. **90:** 522–529.

Browse, J., Mcconn, M., James, D., and Miquel, M. (1993). Mutants of *Arabidopsis* deficient in the synthesis of alpha-linolenate - Biochemical and genetic-characterization of the endoplasmic-reticulum linoleoyl desaturase. J. Biol. Chem. **268:** 16345–16351.

Browse, J., Mccourt, P.J., and Somerville, C.R. (1986a). Fatty-acid composition of leaf lipids determined after combined digestion and fatty-acid methyl-ester formation from fresh tissue. Anal. Biochem. **152:** 141–145.

Browse, J., Warwick, N., Somerville, C.R., and Slack, C.R. (1986b). Fluxes through the prokaryotic and eukaryotic pathways of lipid synthesis in the 16-3 plant *Arabidopsis thaliana.* Biochem. J. **235:** 25–31.

Bucke, C. (1968). Distribution and stability of alpha-tocopherol in subcellular fractions of broad bean leaves. Phytochemistry **7:** 693–700.

Burton, G.W., and Ingold, K.U. (1981). Autoxidation of biological molecules. 1. The antioxidant activity of vitamin-E and related chain-breaking phenolic antioxidants *in vitro.* J. Am. Chem. Soc. **103:** 6472–6477.

Buseman, C.M., Tamura, P., Sparks, A.A., Baughman, E.J., Maatta, S., Zhao, J., Roth, M.R., Esch, S.W., Shah, J., Williams, T.D., and Welti, R. (2006). Wounding stimulates the accumulation of glycerolipids containing oxophytodienoic acid and dinor-oxophytodienoic acid in *Arabidopsis* leaves. Plant Physiol. **142:** 28–39.

Chechetkin, I.R., Medvedeva, N.V., and Grechkin, A.N. (2004). The novel pathway for ketodiene oxylipin biosynthesis in Jerusalem artichoke (*Helianthus tuberosus*) tubers. Biochim. Biophys. Acta **1686:** 7–14.

Collakova, E., and DellaPenna, D. (2001). Isolation and functional analysis of homogentisate phytyltransferase from *Synechocystis* sp. PCC 6803 and *Arabidopsis.* Plant Physiol. **127:** 1113–1124.

Collakova, E., and DellaPenna, D. (2003). Homogentisate phytyltransferase activity is limiting for tocopherol biosynthesis in *Arabidopsis.* Plant Physiol. **131:** 632–642.

Connell, E., Darios, F., Broersen, K., Gatsby, N., Peak-Chew, S.Y., Rickman, C., and Davletov, B. (2007). Mechanism of arachidonic acid action on syntaxin-Munc18. EMBO Rep. **8:** 414–419.

Dahnhardt, D., Falk, J., Appel, J., van der Kooij, T.A.W., Schulz-Friedrich, R., and Krupinska, K. (2002). The hydroxyphenylpyruvate dioxygenase from Synechocystis sp PCC 6803 is not required for plastoquinone biosynthesis. FEBS Lett. **523:** 177–181.

Darios, F., and Davletov, B. (2006). Omega-3 and omega-6 fatty acids stimulate cell membrane expansion by acting on syntaxin 3. Nature **440:** 813–817.

Davletov, B., Connell, E., and Darios, F. (2007). Regulation of SNARE fusion machinery by fatty acids. Cell. Mol. Life Sci. **64:** 1597–1608.

DellaPenna, D., and Pogson, B.J. (2006). Vitamin synthesis in plants: Tocopherols and carotenoids. Annu. Rev. Plant Biol. **57:** 711–738.

Devaiah, S.P., Roth, M.R., Baughman, E., Li, M., Tamura, P., Jeannotte, R., Welti, R., and Wang, X. (2006). Quantitative profiling of polar glycerolipid species from organs of wild-type *Arabidopsis* and a phospholipase Dalpha1 knockout mutant. Phytochemistry **67:** 1907–1924.

DeWitt, G., Richards, J., Mohnen, D., and Jones, A.M. (1999). Comparative compositional analysis of walls with two different morphologies: Archetypical versus transfer-cell-like. Protoplasma **209:** 238–245.

Erin, A.N., Spirin, M.M., Tabidze, L.V., and Kagan, V.E. (1984). Formation of alpha-tocopherol complexes with fatty acids - A hypothetical mechanism of stabilization of biomembranes by vitamin E. Biochim. Biophys. Acta **774:** 96–102.

Esch, S.W., Tamura, P., Sparks, A.A., Roth, M.R., Devaiah, S.P., Heinz, E., Wang, X., Williams, T.D., and Welti, R. (2007). Rapid characterization of fatty acyl composition of complex lipids by collision-induced dissociation time-of-flight mass spectrometry. J. Lipid Res. **48:** 235–241.

Evans, H.M., and Bishop, K.S. (1922). On the existence of a hitherto unrecognized dietary factor essential for reproduction. Science **56:** 650–651.

Fahrenholtz, S.R., Doleiden, F.H., Trozzolo, A.M., and Lamola, A.A. (1974). Quenching of singlet oxygen by alpha-tocopherol. Photochem. Photobiol. **20:** 505–509.

Falcone, D.L., Gibson, S., Lemieux, B., and Somerville, C. (1994). Identification of a gene that complements an *Arabidopsis* mutant deficient in chloroplast omega-6 desaturase activity. Plant Physiol. **106:** 1453–1459.

Farmer, E.E., Almeras, E., and Krishnamurthy, V. (2003). Jasmonates and related oxylipins in plant responses to pathogenesis and herbivory. Curr. Opin. Plant Biol. **6:** 372–378.

Fisk, I.D., White, D.A., Carvalho, A., and Gray, D.A. (2006). Tocopherol - An intrinsic component of sunflower seed oil bodies. J. Am. Oil Chem. Soc. **83:** 341–344.

Fryer, M.J. (1992). The antioxidant effects of thylakoid vitamin E (alpha-tocopherol). Plant Cell Environ. **15:** 381–392.

Hara, A., and Radin, N.S. (1978). Lipid extraction of tissues with a low loxicity solvent. Anal. Biochem. **90:** 420–426.

Harrington, G.N., Franceschi, V.R., Offler, C.E., Patrick, J.W., Tegeder, M., Frommer, W.B., Harper, J.F., and Hitz, W.D. (1997). Cell specific expression of three genes involved in plasma membrane sucrose transport in developing *Vicia faba* seed. Protoplasma **197:** 160–173.

Havaux, M., Eymery, F., Porfirova, S., Rey, P., and Dormann, P. (2005). Vitamin E protects against photoinhibition and photooxidative stress in *Arabidopsis thaliana.* Plant Cell **17:** 3451–3469.

Hofius, D., Hajirezaei, M.R., Geiger, M., Tschiersch, H., Melzer, M., and Sonnewald, U. (2004). RNAi-mediated tocopherol deficiency impairs photoassimilate export in transgenic potato plants. Plant Physiol. **135:** 1256–1268.

Howe, G.A., and Schilmiller, A.L. (2002). Oxylipin metabolism in response to stress. Curr. Opin. Plant Biol. **5:** 230–236.

Hugly, S., and Somerville, C. (1992). A role for membrane lipid polyunsaturation in chloroplast biogenesis at low temperature. Plant Physiol. **99:** 197–202.

Jiang, Q., Elson-Schwab, I., Courtemanche, C., and Ames, B.N. (2000). Gamma-tocopherol and its major metabolite, in contrast to alpha-tocopherol, inhibit cyclooxygenase activity in macrophages and epithelial cells. Proc. Natl. Acad. Sci. USA **97:** 11494–11499.

Kagan, V.E. (1989). Tocopherol stabilizes membrane against phospholipase A, free fatty acids, and lysophospholipids. Ann. N. Y. Acad. Sci. **570:** 121–135.

Kamal-Eldin, A., and Appelqvist, L.A. (1996). The chemistry and antioxidant properties of tocopherols and tocotrienols. Lipids **31:** 671–701.

Latham, C.F., Osborne, S.L., Cryle, M.J., and Meunier, F.A. (2007). Arachidonic acid potentiates exocytosis and allows neuronal SNARE complex to interact with Munc18a. J. Neurochem. **100:** 1543–1554.

Liebler, D.C., and Burr, J.A. (1992). Oxidation of vitamin E during iron-catalyzed lipid peroxidation - Evidence for electron-transfer reactions of the tocopheroxyl radical. Biochemistry **31:** 8278–8284.

Maeda, H., and DellaPenna, D. (2007). Tocopherol functions in photosynthetic organisms. Curr. Opin. Plant Biol. **10:** 260–265.

Maeda, H., Sakuragi, Y., Bryant, D.A., and DellaPenna, D. (2005). Tocopherols protect *Synechocystis* sp strain PCC 6803 from lipid peroxidation. Plant Physiol. **138:** 1422–1435.

Maeda, H., Song, W., Sage, T. L., and DellaPenna, D. (2006). Tocopherols play a crucial role in low temperature adaptation and phloem loading in *Arabidopsis.* Plant Cell **18:** 2710–2732.

Marechal, E., Block, M.A., Dorne, A.J., Douce, R., and Joyard, J. (1997). Lipid synthesis and metabolism in the plastid envelope. Physiol. Plant. **100:** 65–77.

McConn, M., and Browse, J. (1996). The critical requirement for linolenic acid is pollen development, not photosynthesis in an *Arabidopsis* mutant. Plant Cell **8:** 403–416.

McConn, M., Hugly, S., Browse, J., and Somerville, C. (1994). A mutation at the *fad8* locus of *Arabidopsis* identifies a 2nd chloroplast omega-3 desaturase. Plant Physiol. **106:** 1609–1614.

Mène-Saffrané, L., Davoine, C., Stolz, S., Majcherczyk, P., and Farmer, E.E. (2007). Genetic removal of tri-unsaturated fatty acids suppresses developmental and molecular phenotypes of an *Arabidopsis* tocopherol-deficient mutant. Whole-body mapping of malondialdehyde pools in a complex eukaryote. J. Biol. Chem. **282:** 35749–35756.

Miquel, M., and Browse, J. (1992). *Arabidopsis* mutants deficient in polyunsaturated fatty acid synthesis - Biochemical and genetic characterization of a plant oleoyl-phosphatidylcholine desaturase. J. Biol. Chem. **267:** 1502–1509.

Miquel, M., James, D., Dooner, H., and Browse, J. (1993). *Arabidopsis* requires polyunsaturated lipids for low temperature survival. Proc. Natl. Acad. Sci. USA **90:** 6208–6212.

Montillet, J.L., Cacas, J.L., Garnier, L., Montané, M.H., Douki, T., Bessoule, J.J., Polkowska-Kowalczyk, L., Maciejewska, U., Agnel, J.P., Vial, A., and Triantaphylidès, C. (2004). The upstream oxylipin profile of *Arabidopsis thaliana*: A tool to scan for oxidative stresses. Plant J. **40:** 439–451.

Morris, L.J. (1966). Separations of lipids by silver ion chromatography. J. Lipid Res. **7:** 717–732.

Mueller, M.J. (2004). Archetype signals in plants: the phytoprostanes. Curr. Opin. Plant Biol. **7:** 441–448.

Munne-Bosch, S., and Alegre, L. (2002). The function of tocopherols and tocotrienols in plants. Crit. Rev. Plant Sci. **21:** 31–57.

Munne-Bosch, S., and Falk, J. (2004). New insights into the function of tocopherols in plants. Planta **218:** 323–326.

Munne-Bosch, S., Weiler, E.W., Alegre, L., Muller, M., Duchting, P., and Falk, J. (2007). Alpha-tocopherol may influence cellular signaling by modulating jasmonic acid levels in plants. Planta **225:** 681–691.

Offler, C.E., McCurdy, D.W., Patrick, J.W., and Talbot, M.J. (2002). Transfer cells: Cells specialized for a special purpose. Annu. Rev. Plant Biol. **54:** 431–454.

Okuley, J., Lightner, J., Feldmann, K., Yadav, N., Lark, E., and Browse, J. (1994). *Arabidopsis FAD2* gene encodes the enzyme that is essential for polyunsaturated lipid synthesis. Plant Cell **6:** 147–158.

Pentland, A.P., Morrison, A.R., Jacobs, S.C., Hruza, L.L., Hebert, J.S., and Packer, L. (1992). Tocopherol analogs suppress arachidonic-acid metabolism via phospholipase inhibition. J. Biol. Chem. **267:** 15578–15584.

Pollard, M., and Ohlrogge, J. (1999). Testing models of fatty acid transfer and lipid synthesis in spinach leaf using *in vivo* oxygen-18 labeling. Plant Physiol. **121:** 1217–1226.

Porfirova, S., Bergmuller, E., Tropf, S., Lemke, R., and Dormann, P. (2002). Isolation of an *Arabidopsis* mutant lacking vitamin E and identification of a cyclase essential for all tocopherol biosynthesis. Proc. Natl. Acad. Sci. USA **99:** 12495–12500.

Provencher, L.M., Miao, L., Sinha, N., and Lucas, W.J. (2001). *Sucrose export defective1* encodes a novel protein implicated in chloroplast-to-nucleus signaling. Plant Cell **13:** 1127–1141.

Ricciarelli, R., Tasinato, A., Clement, S., Ozer, N.K., Boscoboinik, D., and Azzi, A. (1998). Alpha-tocopherol specifically inactivates cellular protein kinase C alpha by changing its phosphorylation state. Biochem. J. **334:** 243–249.

Ricciarelli, R., Zingg, J.M., and Azzi, A. (2002). The 80th anniversary of vitamin E: Beyond its antioxidant properties. Biol. Chem. **383:** 457–465.

Rimbach, G., Minihane, A.M., Majewicz, J., Fischer, A., Pallauf, J., Virgli, F., and Weinberg, P.D. (2002). Regulation of cell signalling by vitamin E. Proc. Nutr. Soc. **61:** 415–425.

Roughan, P.G., Holland, R., and Slack, C.R. (1980). The role of chloroplasts and microsomal fractions in polar lipid synthesis from [1-14C]acetate by cell free preparations from spinach (*Pinacia oleracea*) leaves. Biochem. J. **188:** 17–24.

Routaboul, J.M., Fischer, S.F., and Browse, J. (2000). Trienoic fatty acids are required to maintain chloroplast function at low temperatures. Plant Physiol. **124:** 1697–1705.

Russin, W.A., Evert, R.F., Vanderveer, P.J., Sharkey, T.D., and Briggs, S.P. (1996). Modification of a specific class of plasmodesmata and loss of sucrose export ability in the *sucrose export defective1* maize mutant. Plant Cell **8:** 645–658.

Sakuragi, Y., Maeda, H., DellaPenna, D., and Bryant, D.A. (2006). α-Tocopherol plays a role in photosynthesis and macronutrient homeostasis of the cyanobacterium Synechocystis sp. PCC 6803 that is independent of its antioxidant function. Plant Physiol. **141:** 508–521.

Sattler, S.E., Cahoon, E.B., Coughlan, S.J., and DellaPenna, D. (2003). Characterization of tocopherol cyclases from higher plants and cyanobacteria. Evolutionary implications for tocopherol synthesis and function. Plant Physiol. **132:** 2184–2195.

Sattler, S.E., Gilliland, L.U., Magallanes-Lundback, M., Pollard, M., and DellaPenna, D. (2004). Vitamin E is essential for seed longevity, and for preventing lipid peroxidation during germination. Plant Cell **16:** 1419–1432.

Sattler, S.E., Mene-Saffrane, L., Farmer, E.E., Krischke, M., Mueller, M.J., and DellaPenna, D. (2006). Nonenzymatic lipid peroxidation reprograms gene expression and activates defense markers in *Arabidopsis* tocopherol-deficient mutants. Plant Cell **18:** 3706–3720.

Savidge, B., Weiss, J.D., Wong, Y.H.H., Lassner, M.W., Mitsky, T.A., Shewmaker, C.K., Post-Beittenmiller, D., and Valentin, H.E. (2002). Isolation and characterization of homogentisate phytyltransferase genes from Synechocystis sp PCC 6803 and *Arabidopsis.* Plant Physiol. **129:** 321–332.

Schmidt, W., Tittel, J., and Schikora, A. (2000). Role of hormones in the induction of iron deficiency responses in *Arabidopsis* roots. Plant Physiol. **122:** 1109–1118.

Schneider, C. (2005). Chemistry and biology of vitamin E. Mol. Nutr. Food Res. **49:** 7–30.

Soll, J., Kemmerling, M., and Schultz, G. (1980). Tocopherol and plastoquinone synthesis in spinach-chloroplasts subfractions. Arch. Biochem. Biophys. **204:** 544–550.

Soll, J., Schultz, G., Joyard, J., Douce, R., and Block, M.A. (1985). Localization and synthesis of prenylquinones in isolated outer and inner envelope membranes from spinach-chloroplasts. Arch. Biochem. Biophys. **238:** 290–299.

Stillwell, W., Dallman, T., Dumaual, A.C., Crump, F.T., and Jenski, L.J. (1996). Cholesterol versus alpha-tocopherol: Effects on properties of bilayers made from heteroacid phosphatidylcholines. Biochemistry **35:** 13353–13362.

Talbot, M.J., Franceschi, V.R., McCurdy, D.W., and Offler, C.E. (2001). Wall ingrowth archtecture in epidermal transfer cells of *Vicia faba* cotyledons. Protoplasma **215:** 191–203.

Talbot, M.J., Offler, C.E., and McCurdy, D.W. (2002). Transfer cell wall architecture: A contribution towards understanding localized wall deposition. Protoplasma **219:** 197–209.

Talbot, M.J., Wasteneys, G.O., Offler, C.E., and McCurdy, D.W.

(2007). Cellulose synthesis is required for deposition of reticulate wall ingrowths in transfer cells. Plant Cell Physiol. **48:** 147–158.

Tappel, A.L. (1972). Vitamin-E and free-radical peroxidation of lipids. Ann. N. Y. Acad. Sci. **203:** 12–28.

Vaughn, K.C., Talbot, M.J., Offler, C.E., and McCurdy, D.W. (2007). Wall ingrowths in epidermal transfer cells of *Vicia faba* cotyledons are modified primary walls marked by localized accumulations of arabio-galactan proteins. Plant Cell Physiol. **48:** 159–168.

Wallis, J.G., and Browse, J. (2002). Mutants of Arabidopsis reveal many roles for membrane lipids. Prog. Lipid Res. **41:** 254–278.

Wang, X.Y., and Quinn, P.J. (2000). The location and function of vitamin E in membranes. review. Mol. Membr. Biol. **17:** 143–156.

Weber, H., Borisjuk, L., Heim, U., Sauer, N., and Wobus, U. (1997). A role for sugar transporters during seed development: Molecular characterization of a hexose and a sucrose carrier in fava bean seeds. Plant Cell **9:** 895–908.

Welti, R., Li, W.Q., Li, M.Y., Sang, Y.M., Biesiada, H., Zhou, H.E., Rajashekar, C.B., Williams, T.D., and Wang, X.M. (2002). Profiling membrane lipids in plant stress responses - Role of phospholipase D alpha in freezing-induced lipid changes in *Arabidopsis.* J. Biol. Chem. **277:** 31994–32002.

Welti, R., and Wang, X.M. (2004). Lipid species profiling: A high-throughput approach to identify lipid compositional changes and determine the function of genes involved in lipid metabolism and signaling. Curr. Opin. Plant Biol. **7:** 337–344.

White, D.A., Fisk, I.D., and Gray, D.A. (2006). Characterisation of oat (*Avena sativa L.*) oil bodies and intrinsically associated E-vitamers. J. Cereal Sci. **43:** 244–249.

Williams, J.P., Khan, M.U., Mitchell, K., and Johnson, G. (1988). The effect of temperature on the level and biosynthesis of unsaturated fatty acids in diacylglycerols of *Brassica napus* leaves. Plant Physiol. **87:** 904–910.

Wise, R.R., and Naylor, A.W. (1987). Chilling-enhanced photooxidation - Evidence for the role of singlet oxygen and superoxide in the breakdown of pigments and endogenous antioxidants. Plant Physiol. **83:** 278–282.

Xu, C.C., Fan, J.L., Riekhof, W., Froehlich, J.E., and Benning, C. (2003). A permease-like protein involved in ER to thylakoid lipid transfer in *Arabidopsis.* EMBO J. **22:** 2370–2379.

Yamauchi, R., and Matsushita, S. (1976). Quantitative changes in tocopherols and their intracellular distribution in cotyledons accompanying with soybean germination. J. Agric. Chem. Soc. Japan **50:** 525–529.